INVESTIGATION OF FLOW PARAMETERS FOR TITANIUM COLD SPRAYING USING CFD SIMULATION

THE UNIVERSITY OF
WAIKATO
Te Whare Wānanga o Waikato

A thesis submitted in partial fulfilment of

the requirement for the degree of

Master in Engineering

at

The Department of Engineering

in

The University of Waikato

by

Tejinder Pal Singh

2010

ABSTRACT

A comprehensive study of cold gas dynamic spray technology is required for optimising performance and gun design for spraying various materials. Cold spraying technology is a new technique in industry and very limited data is available. This thesis focuses on the investigation of cold spray parameters for spraying ductile titanium alloys through a de-Laval convergent-divergent nozzle and optimisation of the nozzle dimensions. This work describes a detailed study of the various parameters, namely applied gas pressure, gas temperature, size of titanium particles and dimensions of the nozzle on the outlet velocity of the titanium particles.

A model of a two-dimensional axisymmetric nozzle was used to generate the flow field of titanium particles with the help of a gas stream flowing at supersonic speed. ANSYS FLUENT software was used for the simulation of a cold spray nozzle. A standard k-ε model has been used to account for the turbulence produced due to the very high velocity flow. Differences in the velocity of titanium particles were modelled over the range of applied gas pressure, gas temperature and size of titanium particles. From the CFD simulation results optimum values of gas pressure and temperature were found for making a successful coating of titanium particles. The optimum nozzle dimensions were also found as the diverging length and exit diameter of the nozzle were found to affect the outlet velocity of titanium particles.

The simulation results show good agreement with previous cold spray work using different spraying materials. Validation of the CFD model was done by referring

to the experimental work and CFD work done for a similar kind of flow field. The grid quality of the model was investigated to get the results to converge and be independent of the grid size to give good agreement between the accuracy of results and the computational time.

ACKNOWLEDGEMENT

Firstly and most importantly, I would like to express my sincere gratitude and appreciation to my supervisor Dr. Brian Gabbitas for his guidance and constant support throughout the work. Also, for making sure that necessary resources were available. His belief in me and friendly nature helped me to complete this thesis.

I wish to express my thanks to Dr. James Neale for letting me use the CFD lab and providing me with the required resources for doing my work. Every member of the energy group carries great competence, knowledge and humour which made great working environment within the CFD lab.

Thanks to PhD. student Jonas Hoffman-Vocke for giving me his precious time and valuable advices and explanations. He has always been there to listen to my problems and help me in any possible ways.

I would also like to thank my parents for their constant support and belief in me and my younger brother Harkirat Singh. Thanks to all my colleagues, close friends for all the good time that enhanced my studies.

Last but not the least, thanks to God's grace.

CONTENTS

ABSTRACT ..... **ii**

ACKNOWLEDGEMENT ..... **iv**

CONTENTS ..... **v**

LIST OF FIGURES ..... **ix**

LIST OF TABLES ..... **xiv**

1 INTRODUCTION **1**

1.1 STRUCTURE OF THESIS 2

2 BACKGROUND **3**

2.1 THERMAL SPRAYING 5

2.2 DIFFERENT METHODS OF THERMAL SPRAYING 6

2.2.1 HVOF 6

2.2.2 ELECTRIC ARC WIRE SPRAYING 7

2.2.3 PLASMA SPRAYING 9

2.2.4 FLAME SPRAYING 9

2.3 COLD SPRAY PROCESS 11

2.3.1 REASON FOR DOING COLD SPRAYING 12

2.3.2 EQUIPMENT USED IN COLD SPRAYING 15

2.4 FACTORS EFFECTING THE COLD SPRAY PROCESS 19

2.4.1 EFFECT OF GAS TEMPERATURE 19

2.4.2 EFFECT OF GAS PRESSURE 23

2.4.3 THE EFFECT OF THE TYPE OF GAS 25

2.4.4 THE EFFECT OF PARTICLE SIZE 29

2.5 DE-LAVAL NOZZLE 32

2.5.1 BACKGROUND OF THE DE-LAVAL NOZZLE 32

2.5.2 REASON FOR USING A DE-LAVAL NOZZLE 33

2.6 OPTIMIZATION OF NOZZLE DESIGN 37

2.6.1 EFFECT OF THE DIVERGENT LENGTH ON THE OPTIMIZATION OF THE NOZZLE EXIT 38

2.6.2 OPTIMIZATION OF THE NOZZLE EXIT DIAMETER 38

2.7 SIMULATION OF COLD SPRAY PROCESS 39

3 EXPERIMENTAL PROCEDURE 42

3.1 INTRODUCTION TO CFD 42

3.1.1 REASON FOR USING CFD 43

3.2 INTRODUCTION TO FLUENT 45

3.2.1 CFD VALIDATION 47

3.3 MODEL GENERATION OF NOZZLE IN GAMBIT 47

3.4 EXPERIMENTAL PROCEDURE..... 49

3.4.1 MESH GENERATION..... 50

3.5 COMPUTATIONAL RESOURCES AND TIME 53

3.6 MODEL PARAMETERS 54

3.6.1 SECOND ORDER SCHEME..... 54

3.7 TURBULENCE MODELLING..... 55

3.8 BOUNDARY AND INITIAL CONDITIONS..... 57

3.8.1 FLOW FIELD 58

3.8.2 FLUID PROPERTIES 60

3.8.3 DISCRETE PHASE MODELLING 61

3.9 ASSUMPTIONS 61

3.10 CONVERGENCE ASSESMENT 62

4 RESULTS AND DISCUSSIONS 63

4.1 FLOW OF CARRIER GAS INSIDE THE NOZZLE..... 63

4.1.1 EFFECT OF PRESSURE AND TEMPERATURE ON VELOCITY OF GAS..... 65

4.2 EFFECT OF TITANIUM PARTICLE SIZE ON EXIT VELOCITY ... 68

4.3 EFFECT OF THE CARRIER GAS ON PARTICLE VELOCITY 72

4.4 EFFECT OF GAS CONDITION ON VELOCITY OF TITANIUM PARTICLES 73

4.4.1 EFFECT OF GAS TEMPERATURE ON PARTICLE VELOCITY 73

4.4.2 AFFECT OF THE GAS TEMPERATURE ON THE PARTICLE TEMPERATURE..... 74

4.4.3 AFFECT OF INITIAL PRESSURE ON THE VELOCITY OF TITANIUM PARTICLES..... 75

4.5 EFFECT OF THE NOZZLE DESIGN ON THE VELOCITY OF TITANIUM PARTICLES..... 77

4.5.1 EFFECT OF THE DIVERGENT LENGTH..... 77

4.5.2 EFFECT OF NOZZLE EXIT DIAMETER..... 79

4.6 CONCLUSIONS..... 81

REFERENCES..... 83

APPENDIX 1..... 93

APPENDIX 2..... 95

LIST OF FIGURES

Figure 1: Number of patents applications over the number of years [8] 4

Figure 2: Schematic diagram of HVOF apparatus [17] 7

Figure 3: Schematic diagram of electric arc wire spraying system [15]..... 8

Figure 4: Schematic diagram of plasma spraying system [17] 9

Figure 5: Schematic diagram of HVSFS torch 10

Figure 6: Schematic diagram of cold spraying system 11

Figure 7: Correlation between the particle velocity and deposition efficiency 12

Figure 8: Value stream analysis [4] 13

Figure 9: The block diagram of cold spray system [27] 15

Figure 10: The cold spray system in ASB Industry, Inc [4] 15

Figure 11: Effect of the nitrogen temperature on particle velocity and temperature under a pressure of 1.4 MPa..... 20

Figure 12: Effect of the nitrogen temperature on particle velocity and temperature under a pressure of 1.4 MPa [5]..... 20

Figure 13: A spray gun developed by the CGT spray system..... 21

Figure 14: Critical particle impact velocity as a function of particle temperature, with an optimum window of impact conditions [3]..... 22

Figure 15: Effect of N_2 temperature on deposition efficiency [6]..... 22

Figure 16: Dependence of deposition efficiency of coating on gas pressure [7].. 23

Figure 17: Effect of gas pressure on particle velocity [8]..... 24

Figure 18: High pressure system..... 25

Figure 19: Low pressure system 25

Figure 20: Comparison between measure average particle velocity and predicted average particle velocity using ●: Helium, 24 bars. ♦: Helium, 20 bars [15]..... 27

Figure 21: Comparison between measure average particle velocity and predicted average particle velocity using ▲: Nitrogen, 24 bars. ■: Nitrogen, 20 bars [15]. 27

Figure 22: The mean particle velocity versus z-axis position (x = 0, y= 0). 22 μm copper particles powder; 200 °C, 2.1 MPa helium or air as driving gas [8]..... 28

Figure 23: The effect of particle diameter on particle velocity under He and N_2 gases operated at the inlet pressure of 2 MPa and temperature of 340 °C [18].... 30

Figure 24: The influence of particle size on particle velocity and particle temperature [20]..... 31

Figure 25: Velocity plot along the nozzle axis [21]..... 32

Figure 26: Diagram of de-Laval nozzle 33

Figure 27: Calculated critical velocities for various spray materials [23] 36

Figure 28: Effect of divergent length on optimal nozzle exit diameter [30]..... 38

Figure 29: Effect of nozzle exit diameter on the velocity of particles with different sizes using nitrogen at pressure 2 MPa and temperature 300 °C [2] 39

Figure 30: Typical model of nozzle used in simulations [29] 41

Figure 31: Example of mesh used for simulations [29] 41

Figure 32: Flow chart of simulation in FLUENT 46

Figure 33: User interface of GAMBIT 48

Figure 34: Model of axisymmetric nozzle drawn in GAMBIT 49

Figure 35: The outlet velocity of the nozzle using different mesh resolutions 51

Figure 36: Sample of the mesh of the inlet of the nozzle 52

Figure 37: Sample of mesh of the throat of the nozzle 52

Figure 38: Sample of the mesh quality 53

Figure 39: Boundary type of the converging part of nozzle 57

Figure 40: Boundary type of the diverging part of the nozzle 58

Figure 41: Plot of convergence monitor in FLUENT 62

Figure 42: Velocity contour plot using air as carrier gas 63

Figure 43: Velocity contour plot using nitrogen as carrier gas 64

Figure 44: Velocity contour plot using helium as carrier gas 64

Figure 45: Profile of static pressure and Mach number distribution along the nozzle axis 65

Figure 46: Effect of temperature and on exit velocity when applied gas pressure was 1.5 MPa 66

Figure 47: Effect of temperature on exit velocity when applied gas pressure was 2.3 MPa 66

Figure 48: Effect of temperature on exit velocity when applied gas pressure was 3.1 MPa 67

Figure 49: Effect of particle size on its velocity 68

Figure 50: Optimum size range for successful bonding of titanium as spray material..... 70

Figure 51: Flow pattern of titanium particles size of 10 μm, 20 μm, 35 μm and 50 μm inside the nozzle using helium as carrier gas at 1.5 MPa and 300 K..... 71

Figure 52: Effect of the carrier gas on titanium particle velocity at applied gas pressure of 2.7 MPa and gas temperature of 600 K 72

Figure 53: Effect of gas temperature on the velocity of titanium particles..... 73

Figure 54: Influence of the particle diameter on the velocity and temperature of the titanium particles..... 74

Figure 55: Effect of gas pressure on the particle velocity with different particle size at temperature of 500 K 76

Figure 56: Model of convergent-divergent nozzle used for simulations 77

Figure 57: Effect of divergent lengths on the gas velocity 78

Figure 58: Effect of the nozzle divergent length on the particle velocity..... 78

Figure 59: Effect of nozzle exit diameter on the gas velocity..... 80

Figure 60: Effect of nozzle exit diameter on the velocity of titanium particles.... 80

LIST OF TABLES

Table 1: The average particle velocity for two cases were found to be 260 and 325 m/s respectively [41].....24

Table 2: Dimensions of nozzle used for modelling.....49

Table 3: Different mesh sizes for the computational domain.....51

Table 4: Table of mass flow rate (kg/sec) of air, nitrogen and helium at 300 K...59

Table 5: Table of thermophysical properties of titanium assumed in simulation are.....69

1 INTRODUCTION

Cold spray process is a new technique for coating metals like copper, aluminium, titanium, gold, etc. on metal substrate. The worldwide interest in this technique has lead to significant research effort both in the design of equipment and methods to make it simple and more efficient. This method is totally different from other coating processes because low temperatures are used and this prevents phase changes in metals and change in few properties like stress generation after the significant change in the temperature. In this process a compressed gas is used as a carrier gas for transporting metal particles through convergent-divergent nozzle which is designed so that the gas, and hence particles, reach supersonic speed. The large amount of plastic deformation in the particles on impact with the substrate causes particles adhesion and deposition of a coating.

The basic cold spray system consists of a compressor, powder feeder, gas heater, nozzle and a control panel to control the gas pressure, powder feed rate and gas temperature. The main principle of the cold spray process is that the coating depends upon the velocity by which particles strike the substrate, because to make a coating the kinetic velocity of sprayed particles should be more than a critical velocity, so a most important aspect of cold spraying is how to get the required kinetic velocity.

The size of the spray particles, gas temperature and gas pressure play an important part in making a coating but the required velocity depends on design of nozzle. Important parameters are the diameter of throat, the diameter of nozzle inlet and outlet, the length of the convergent and divergent parts of the nozzle, because to get supersonic speed we have to use a De Laval convergent-divergent nozzle. We can change the gas pressure, gas temperature and powder feed rate during the

process but we cannot change the dimensions of the nozzle to change the speed or to get maximum efficiency.

So the main aim of this project is to optimize the appropriate nozzle for the cold spray process using CFD (computational fluid dynamics) code the ANSYS FLUENT software of interest is the effect of changes in gas temperature, gas pressure, titanium powder particles size and transportation gas on the exit velocity of titanium particles.

1.1 STRUCTURE OF THESIS

Chapter 1 is an introduction on the cold spray process and its basic principles. It gives the scope of this project.

Chapter 2 outlines the background to cold spray technology and describes past and current research on cold spraying. This chapter also describes the purpose of cold spraying, the equipments used for coating, and the effects of different parameters on the particle velocity. The chapter includes information about the de Laval nozzle, its importance and design.

Chapter 3 presents the experimental set up for spraying titanium particles through a convergent-divergent nozzle using computational fluid dynamics. FLUENT code has been used for flow simulation. Numeric scheme and computational domain grid generation procedure is described in this chapter.

Chapter 4 shows the results of CFD studies. The aim of this work was to analyse changes in flow velocity of titanium particles and affect of various flow parameters on it.

2 BACKGROUND

Over the past few years new spraying techniques have been computationally analysed and modelled for better understanding of the thermo-mechanical processes involved. Cold spray technology is attracting the researchers and industries worldwide because of its advantages over the other spraying methods [1]. The cold spray dynamic technology is a new technique for coating metals with very small metal powder particles using compressed gas stream propulsion. This technology was developed with the aim of producing pore free and non oxidized coatings which were not possible with other conventional coating techniques like HVOF, Plasma spraying and arc spraying. Due to the high velocity of particles, this process gives a highly bonded coating with good adhesion between particles and substrate, low friction coefficient, high thermal and electrical conductivity, and excellent corrosion and oxidation resistance [2].

Many companies and researchers worldwide are working on cold spray. In the USA, research on cold spray technology was first undertaken by a consortium formed under the auspices of the National Centre for Manufacturing Sciences (NCMS). After that many research centres became interested in this technology e.g. the Institute of Theoretical and Applied Mechanics of the Russian Academy of Science, Sandia National Laboratories and Pennsylvania State University [3]. Sandia National Lab had funded companies like ASB Industries, Ford, K-Tech, Pratt & Whitney to a value of 0.5 million U.S. dollars a year for 3 years to do R&D and develop this technology. Pennsylvania State University have received grants from the U.S. Navy to do R&D on the cold spray process and develop an anti skid coating [4].

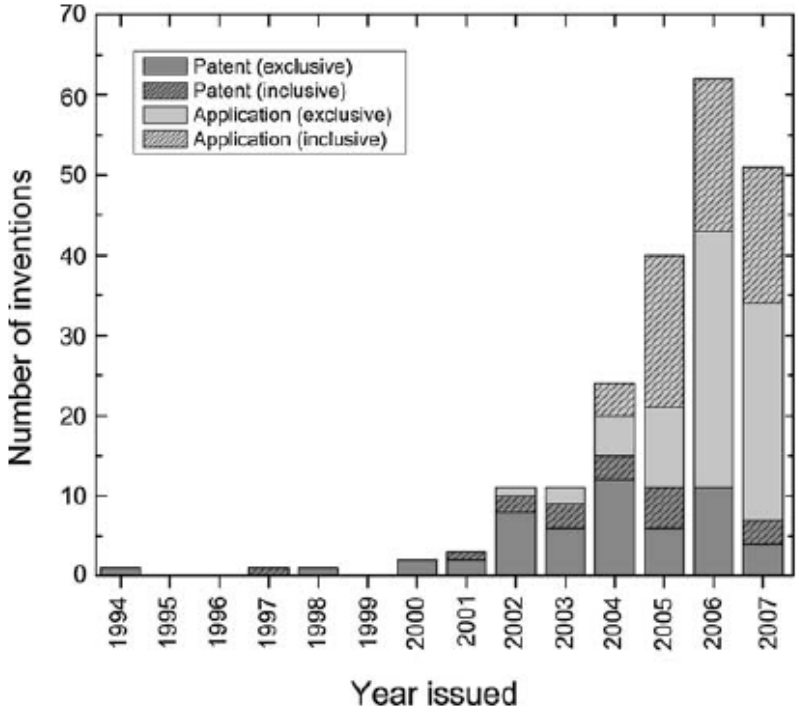

Figure 1: Number of patents applications over the number of years [8]

The above graph shows number of US patents applications inclusive and exclusive to cold spray technology. The exclusive patents refer to patents that protect an idea that uses exclusively cold spray as part of an invention while inclusive patents refer to those patents that include cold spray as one of the many coating technologies [8].

A financial outlay of $3.4 million was spent by a joint venture of McGill University and the National Research Council Canada to do research on this solid-state coating technology [5]. Prof William O'Neil of Cambridge University has received a large grant of about £2 million for research and development on cold spray and the development of manufacturing tools and equipment used in this process [4]. In Australia CSIRO has established a well equipped cold spray

laboratory to initialize this technology and develop it for industrial applications. The Research Program Leader of CSIRO Material Science and Engineering is Dr Mahnaz Jahedi [6].

2.1 THERMAL SPRAYING

Thermal spray is the process in which a metal or alloy in molten or semi molten state is used to make a layer on a substrate. The thermal spray technique was first used in the early 1900s when Dr Schoop (refer to the Master patent of Schoop technology) [9] used a flame as a heat source. Initially it was practiced on metals with low melting point and after that it was progressively extended to metals with high melting point [9]. For making the deposit in thermal spraying a stream of molten metal particles strike a substrate, become flattened and then undergo rapid solidification and quenching. Every droplet spreads to make its own layer and these layers join to make a deposit of thermally sprayed material. In this process voids are formed in the deposit mainly because of incomplete filling or incomplete wetting of the molten metal and during the quenching of brittle materials micro cracks are formed after the solidification of molten material. These affect the mechanical properties like elastic modulus and stress at failure and physical properties like thermal conductivity [10].

When thermal spray is used to make a coating of molten metal on a substrate it results in a phase change and a microstructure with varying degrees of porosity, solidification stresses and poor corrosion resistance [7]. At present thermal spray technology is used by many industries as a basic process for producing a coating with good corrosion resistance, good wear characteristics and thermal barrier

coatings. During thermal spraying the feedstock powder has to be fully or partially molten and the coating is laid-up on the substrate as multi layers. In the case of oxygen sensitive materials thermal spraying is used in a vacuum chamber which increases the cost. Thermal spraying is no good for those materials which readily oxidise or are temperature sensitive [8]. For these materials an option is cold spraying.

2.2 DIFFERENT METHODS OF THERMAL SPRAYING

There are different types of thermal spray methods available to make coatings on a substrate, either to improve surface properties for protection against corrosion, wear or as a thermal barrier. The different types of thermal spraying techniques are:-

1. HVOF (High velocity oxy-fuel spraying)
2. ELECTRIC ARC WIRE SPRAYING
3. PLASMA SPRAYING
4. FLAME SPRAYING
5. COLD SPRAYING [11][12]

2.2.1 HVOF

High velocity oxy-fuel spraying is a method in which oxygen and fuel are burnt and then passed through a nozzle with free expansion which results in a supersonic flame gas velocity. By introducing feedstock powder in the hot stream, the powder particles become extremely hot and reach supersonic velocity. The

particles flatten after striking the substrate to form a well bonded and dense coating [13].

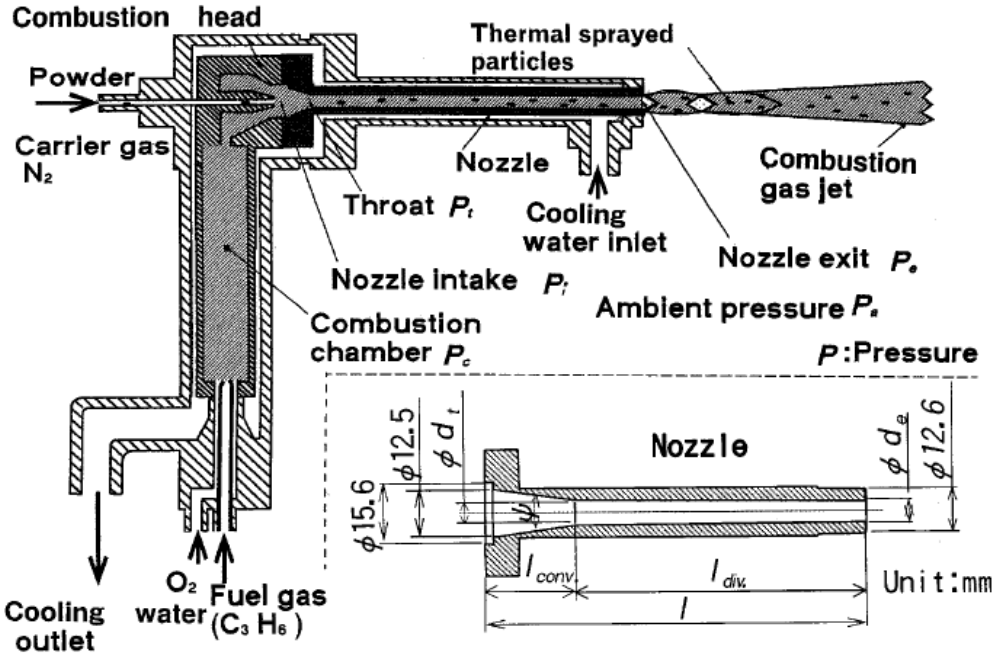

Figure 2: Schematic diagram of HVOF apparatus [17]

As, the temperature of the particles impacting on the substrate ranges from 1500 to 2500 K there is thermal degradation of the coating material. It is difficult to control the temperature of the hot jet and its velocity independently and also difficult to optimize the spray parameters because the spraying parameters, such as fuel flow rate, take time to set up [14].

2.2.2 ELECTRIC ARC WIRE SPRAYING

Electric arc wire spraying is a very useful process for making metal coatings because it is a low cost process. The wire used for welding can be electric arc sprayed at high throughput (from 30 to 50kg/hr) [13].

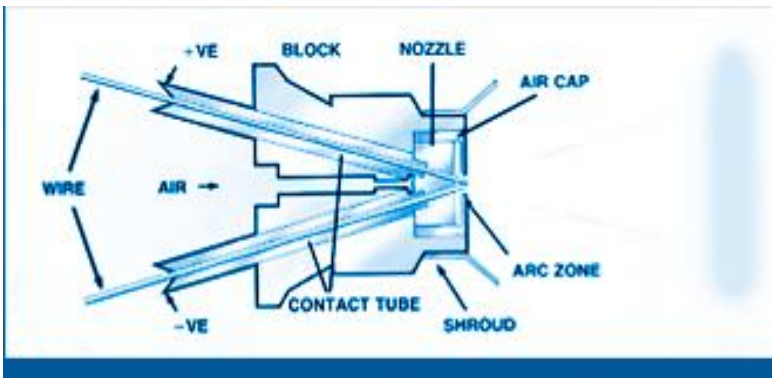

Figure 3: Schematic diagram of electric arc wire spraying system [15]

Two wires are used in these processes, which are electrically charged, one positively and the other negatively by passing a current through them. The wires are joined to make an arc which melts the wires. Compressed air coming from the nozzle reduces the molten metal to tiny particles and sprays them on the substrate. A higher spray rate can be achieved by using a high current rating system like 350A or 700A [15]. The coating formed by this method has relatively high density and adheres well to the work piece. Greater density and more bond strength can be achieved by carrying out the process in a reduced-pressure chamber [13]. The disadvantage of this process is that only wires that are electrically conductive can be used and if preheating of the work piece is required then a separate source is necessary in this task [17].

2.2.3 PLASMA SPRAYING

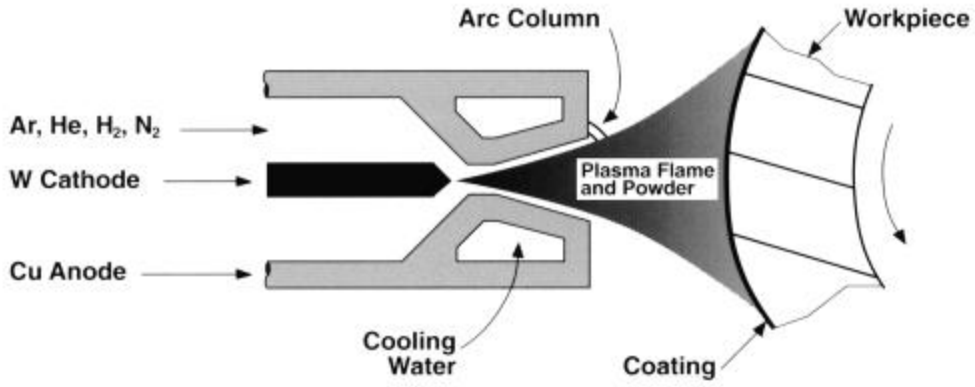

Figure 4: Schematic diagram of plasma spraying system [17]

As we can see in the Figure 4 the nozzle comprises a tungsten cathode placed axially at the outer part of the anode which is a copper cylinder. A direct current arc is maintained between the axially placed tungsten cathode and the copper anode. An ionised gas is generated by heating it up to a temperature of 50,000°F (30,000°C). The powder is then introduced into the plasma jet where it is heated above its melting temperature and achieves a velocity ranging from 120 to 610 m/sec. [17] The behaviour of the plasma spraying process is non-deterministic in which molten, semi-molten or sometimes solid particles strike the substrate, flatten followed by solidification and formation of disc-like splats. The size, velocity and thermo physical properties of the particles striking the surface totally influences the splat shape and hence the quality of the coating [18].

2.2.4 FLAME SPRAYING

Standard spraying techniques have certain limitations. It is difficult to make a thin coating on a substrate as in some techniques only certain sizes of powder particles can be used and cannot be reduced from that size, so it is not easy to achieve a

homogenous and dense coating. A very good powder feeding technique is needed when using powder particle sizes below 5 μm and these powder qualities are very expensive. Not every combination of material is available in the market [19].

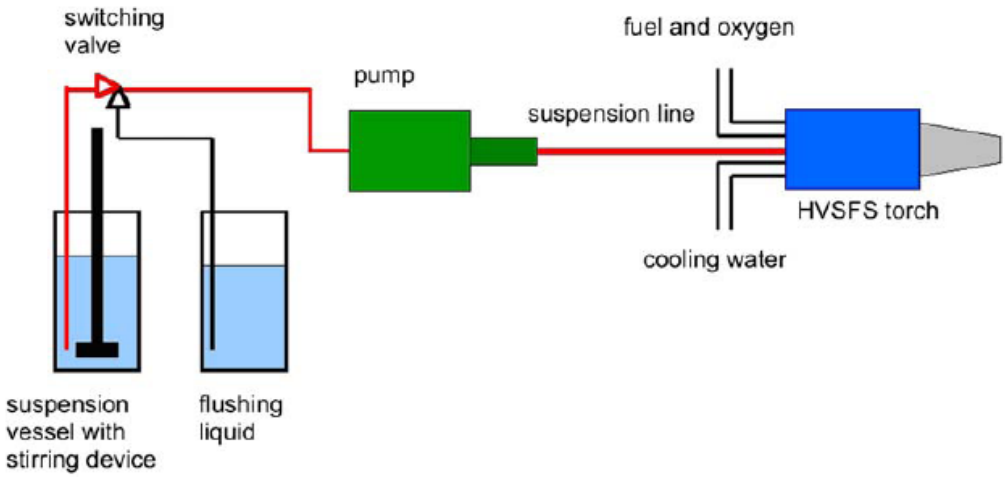

Figure 5: Schematic diagram of HVSFS torch

High velocity suspension flame spraying is a technique used to spray submicron or nanoparticles at hypersonic speed to get a dense and thin coating on a work piece. In this process, the powder is mixed with an organic solvent and fed axially into the combustion chamber or the torch which resembles the High Velocity Oxy-Fuel (HVOF) spray torch [20]. The disadvantage of the HVSFS technique is that for spraying sub-micron sized particles the stand-off distance of the spraying torch has to be very small, which results in heat transfer from the gas jet to the work piece. This heat changes the properties of the piece, so a proper and effective cooling system is required in this process when coating heat sensitive materials [21].

2.3 COLD SPRAY PROCESS

The phenomenon of cold spray was discovered during an aeronautical investigation in the 1980's. When dusty gases were used in shock tube experiments, the particles were observed to stick on the substrate. This process was undesirable but was recognised to be useful because particles of ductile metals or alloys could be bonded onto metal surfaces, glass or ceramics at impact velocities ranging from 400 to 1200 m/s. This is how coatings are made on work pieces [22]. The cold spray process or cold gas-dynamic process is a coating process utilizing high speed metal or alloy particles ranging from 1 to 50 μm in size, with a supersonic jet of compressed gas with a velocity ranging from 300 to 1200 m/s on the surface of the work piece. The coating formed by this process depends upon a combination of factors like particle velocity, temperature and size. The powder particles in this process are accelerated by a supersonic gas jet at a temperature lower than its melting point, thus reducing many effects which occur in high temperature spraying like oxidation at high temperature, melting of the substrate or spray particles, crystallization, evaporation, stress generation, gas release and other related problems [23].

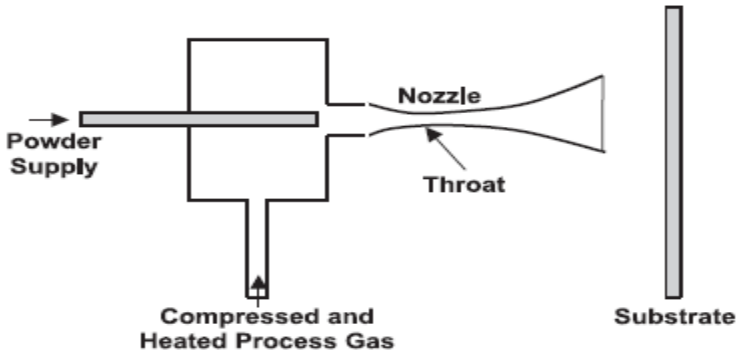

Figure 6: Schematic diagram of cold spraying system

Studies on cold spraying show that the most important parameter is the velocity of the particles before they strike the substrate. For making a successful coating the particles should strike the substrate at a higher velocity than a critical velocity [25].

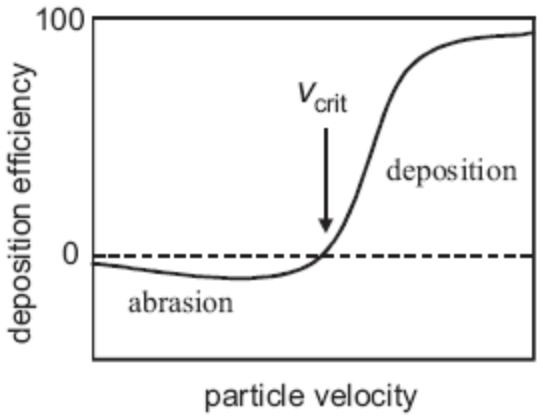

Figure 7: Correlation between the particle velocity and deposition efficiency

If the particles strike the substrate at a velocity lower than the critical velocity then the particles will just scratch the surface of the substrate as they do in grit blasting. By increasing the particle velocity the deposition efficiency reaches saturation point which is nearer to 100%. Most of the research related to cold spray is focused on achieving high particle velocity by making new designs of the nozzle used for spraying [25].

2.3.1 REASON FOR DOING COLD SPRAYING

In the cold spray process, particles ranging in size from 5 to 50μm are used to make a coating by number of layers. The cold spray process is relatively better for making thicker coatings than thermal spraying because there are no thermal stresses involved in it [26].

A most important consideration in introducing new process to industry is a reduction in the manufacturing cost of components. Most components in industry are fabricated by casting which is the initial step in the production line. The Pratt & Whitney company as a part of the US Air Force forging supplier has developed a model called value stream analysis which shows that reduction in cost cannot be achieved by reducing the cost of one area in a production line. Pratt & Whitney also developed a model for Laser Powder Deposition of titanium and this model has been extended to model the cold spray process for titanium [4].

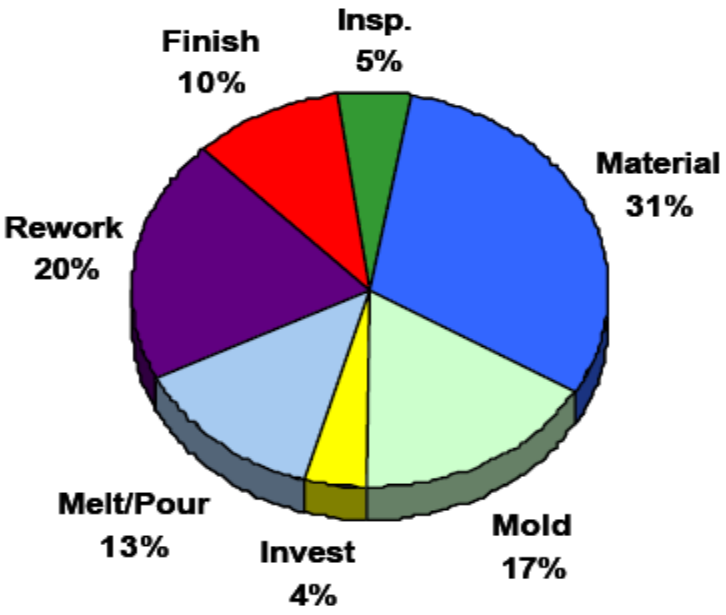

Figure 8: Value stream analysis [4]

The Value Stream Analysis shows that by using the cold spray process reduction in cost can be achieved in the following areas:-

1) Material input

2) Reduction in finishing time

3) Reduction in rework time

4) Reduction in the cost of mould preparation and melt pouring

5) Increase in material utilization because the deposition efficiency in cold spraying is 60 to 95% [4]

The Value Stream results showed that 70% of the value stream could be achieved if rework and finishing were reduced by 75%, material input reduced by 50%, and mould, casting cost and melt/pour cost reduced by 70%. These estimated figures show that it is advantageous to use a cold spray process because of a reduction in the manufacturing cost of components. [4] For example, in the production of large ring rollings and billets made from titanium alloys. Titanium is a very hard material and it can take many days to machine each piece. The process wears out many of the cutting tools and more than 90% of the material is machined away in getting the final product. This can cost more than $ 1 million dollars apiece. Even in large scale production there can be a long lead time because of the limited availability of titanium, the processing capacity and the considerable time to convert stock material into final product, so the cold spray process is used to manufacture near net shapes by depositing titanium alloys [27].

To compare the cost of applying a coating in by cold spraying with other thermal spraying processes a new software package Cost Analysis Software (CAS) is used. This software has been developed for accurately calculating the cost of applying coatings which includes the cost of powder, gas, electricity, nozzle dimensions, desired coating thickness, deposition efficiency and start up and shut

down time. The output includes cost by category (gas, powder, labour, burden, and amortization), cost per unit area, and spray time [28].

2.3.2 EQUIPMENT USED IN COLD SPRAYING

A block diagram of cold spray equipment with a powder heater installed is shown in figure

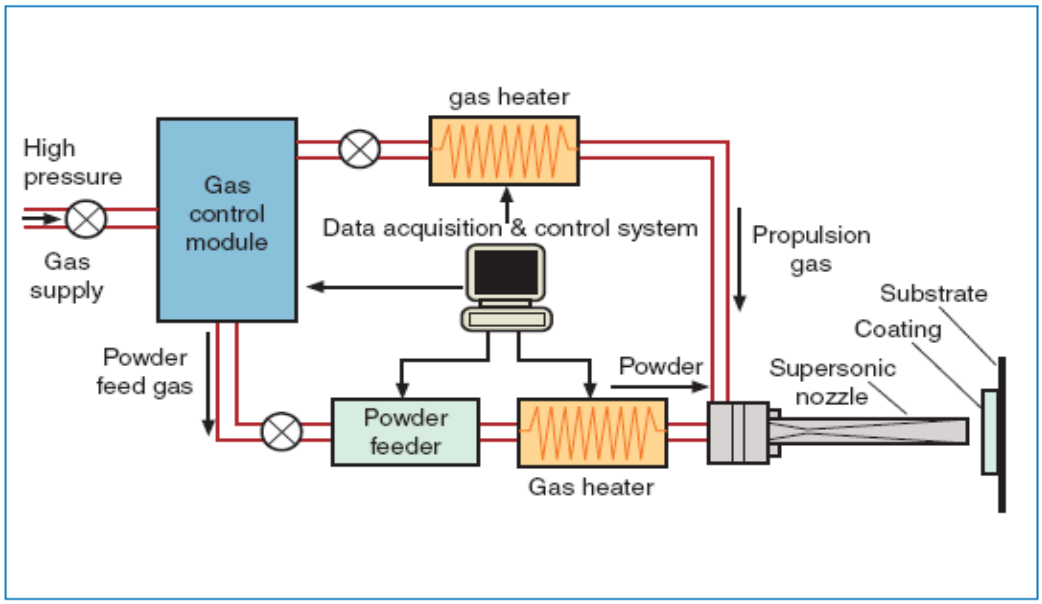

Figure 9: The block diagram of cold spray system [27]

Figure 10: The cold spray system in ASB Industry, Inc [4]

The main parts of the cold spray system involves

- A gas control module which contains the working gases such as helium, nitrogen, argon and mixes of these gases and which enter the nozzle at high pressure.

- A data acquisition and control system for controlling the gas pressure from the compressor, the powder feed rate into the nozzle and the gas heater that maintains the proper temperature of the gas.[29]

- A powder feeder which delivers powder in a continuous flow at a mass rate between 5 to 10 Kg/hr to make a uniform coating and improve reliability for measuring deposition efficiency. The powder feeders currently available come with features like low maintenance, uniform and accurate powder feeding, low powder wastage, minimal pulsing and easy cleaning. [23]

- A gas heater is used to heat the gas up to a temperature ranging from 300° to 650° C before it enters the nozzle. Heating the gas eventually increases the powder particles temperature and velocity and hence ensures plastic deformation after they strike a substrate. However the gas temperature at the inlet of the nozzle is below melting point which means particles do not melt during the process. [30]

- In the coating process, the nozzle is the main component for depositing solid-state particles. In the cold spray process, a convergent-divergent de Laval-type nozzle is used to accelerate the particles at supersonic speed by the gas flow. After leaving the nozzle at high velocity, the particles impinge on the work piece and undergo plastic deformation because of

collision and bonding with the work piece surface and other particles to make a coating. Studies show reference [31] that better injection through the nozzle gives the following benefits in coating formation: -

a) It enables the use of an increased gas temperature for the high cold spray process.

b) The dwell time of the sprayed particles can be increased before they enter the convergent divergent nozzle and heat the particle.

c) More powder gas flow can be used without clogging the nozzle hence increasing the effective temperature of propellant gas [31].

The table below is the typical cold spray control sheet: [32]

VENDOR:	Sheet ___ of ___
VENDOR PROCESS #:	
PURCHASE ORDER NUMBER:	
PART NUMBER:	S/N:
AREA TO RECEIVE DEPOSITION:	
COLD SPRAY (CS) MANUFACTURER:	
PART MATERIAL:	
CS TYPE:	NOZZLE:
PART PREPARATION	
METHOD OF CLEANING:	
MASKING INFORMATION:	
GRIT TYPE AND SIZE:	
GRIT BLAST PRESSURE (MPa) : _____ ± Suction : _____ Pressure : _____	
GAS (1) PRIMARY:	Temperature Deg. C _____ ±
Main Gas Pressure MPa _____ ±	Main Gas Flow (1) m^3/hour. _____ ±
Feeder Gas Pressure MPa _____ ±	Feeder Gas Flow (2) m^3/hour. _____ ±
COATING POWDER	
Powder material: _____	Powder size: _____
Supplier: _____	Material Lot # : _____
COATING DATA	
Elapsed Time Between Surface Prep and Spraying: _____	
Powder Feed Rate (kg/hr): _____	
Powder Meter Wheel: _____	
Nozzle to Work Distance: _____	
Traverse rate (mm/s): _____ Increment (mm): _____	Preheat Temp:
Deposition Thickness as Sprayed:	Method of Preheat:
Number of Passes Per Layer:	Number of Layers:
Method of Cooling (if any): _____	
NOTES:	
CERTIFICATION #: _____	
APPROVAL: _____	

2.4 FACTORS EFFECTING THE COLD SPRAY PROCESS

Recent research on the cold spray process shows that successful coating formation on a substrate depends upon the velocity of the particles exiting the nozzle and striking the surface of work piece. The velocity further depends upon factors such as gas temperature, gas pressure, type of gas used [33], the size of the particles used for spraying and the nozzle design which includes the throat diameter, inlet diameter, outlet diameter, convergent length of nozzle and divergent length [34].

2.4.1 EFFECT OF GAS TEMPERATURE

Previous studies have found that if the temperature of the carrier gas is increased then it directly affects the velocity of the particles [35] and it also results in more deposition efficiency of the particles on the substrate. Compressed gas enters the convergent divergent nozzle with an inlet pressure of around 30 bar to get the supersonic velocity. The solid powder particles are introduced in the nozzle upstream and are accelerated by the rapidly expanding gas in the divergent part of the nozzle. The carrier gas is often preheated to get high gas flow velocities through the nozzle. In the cold spray process the gas is first heated to a temperature ranging from 300 K to 900 K. Particles when introduced into a hot gas stream, are in contact with the gas for a shorter time, so that when the gas expands in the divergent part its temperature decreases. In this process the temperature of the particles remains below their melting temperature [36].

The main gases which are used for cold spraying are helium and nitrogen because of their lower specific weight. Wen-Ya Li *et al* [37] performed an experiment to find the effect of gas conditions on particle velocity and temperature. The experimental results show graphically the effect of inlet temperature of the nitrogen gas on particle velocity when the nitrogen pressure is 1.4 MPa and the effect of helium inlet temperature on particles when the helium pressure is 0.6 MPa.

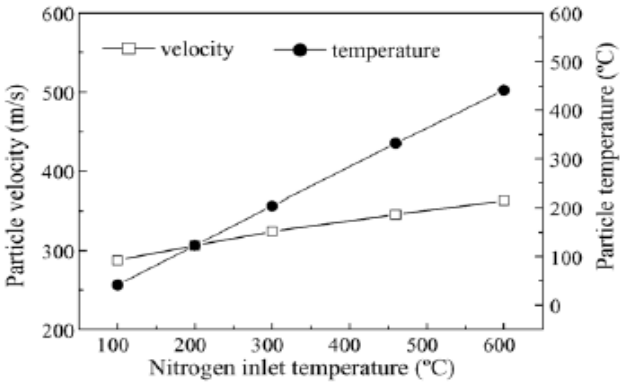

Figure 11: Effect of the nitrogen temperature on particle velocity and temperature under a pressure of 1.4 MPa

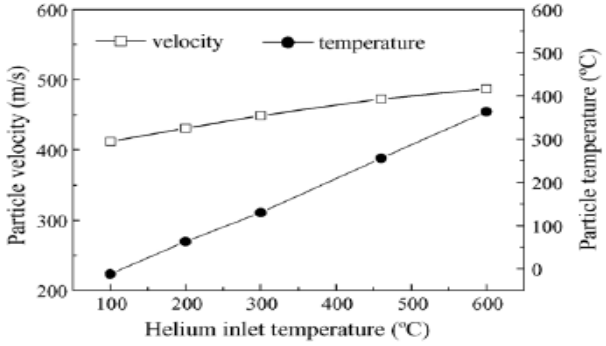

Figure 12: Effect of the nitrogen temperature on particle velocity and temperature under a pressure of 1.4 MPa [37]

The experiment also showed that, particles attained a higher velocity using helium rather than nitrogen at a lower pressure than that used for nitrogen. This is because of the lower molecular weight of helium and larger specific heat ratio [37].

The main consideration arising from increasing the temperature of the gas is the robustness of the nozzle material, which results in getting limited particle velocity and temperature. The German company CGT commercially manufactured a tungsten carbide MOC-nozzle which can spray copper particles at 600° C at a pressure of 30 bars without plugging and erosion of the nozzle material [35].

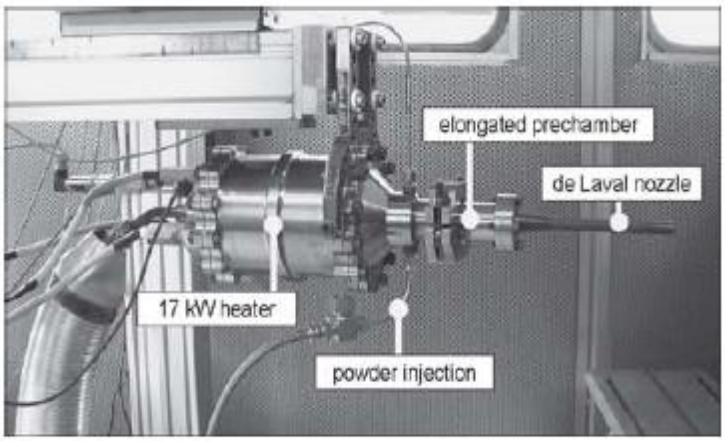

Figure 13: A spray gun developed by the CGT spray system [35]

The main advantage of a high impact temperature is that it decreases the critical velocity of the spray material because of thermal softening. The Figure 14 shows the two lines which indicate the critical velocity and erosion velocities. Both are temperature independent [35].

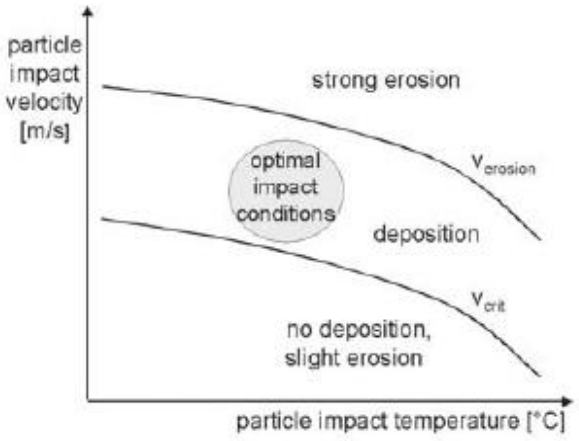

Figure 14: Critical particle impact velocity as a function of particle temperature, with an optimum window of impact conditions [35]

The deposition efficiency also depends upon the temperature of the carrier gas. It was found that when nitrogen is used to spray titanium particles the critical temperature is 155 °C, below this temperature no particle deposition took place. When the temperature was further increased from this critical temperature, the deposition efficiency also increased quickly, especially when the temperature of nitrogen exceeded 215 °C [38].

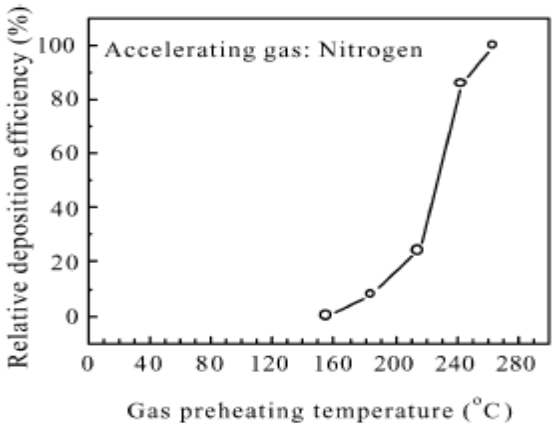

Figure 15: Effect of N_2 temperature on deposition efficiency [38]

2.4.2 EFFECT OF GAS PRESSURE

In an experiment performed by M. Fukumoto *et al* [39] the effect of the gas inlet pressure on the deposition efficiency was investigated and the results showed that deposition efficiency increases with increase in the gas pressure.

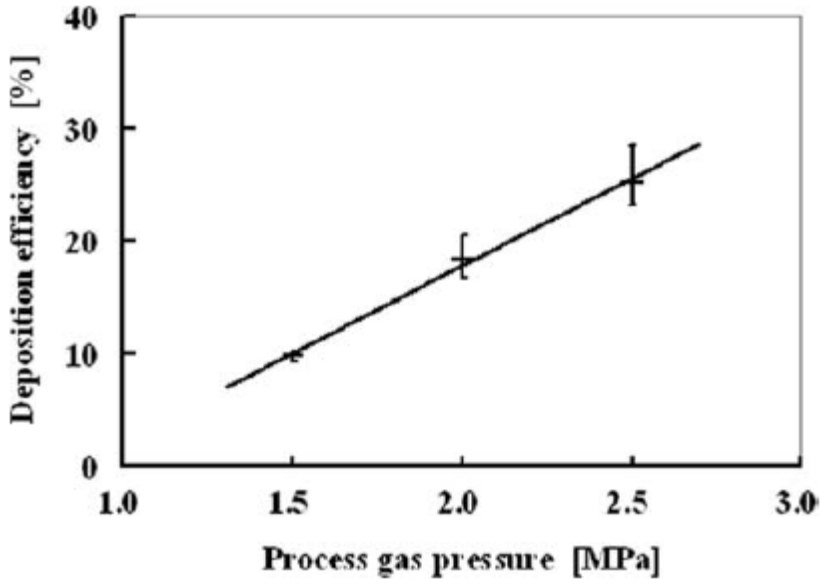

Figure 16: Dependence of deposition efficiency of coating on gas pressure [39]

After studying the supersonic behaviour of the gas spray particles it was found that particle velocity increases with an increase in stagnation pressure [40]. When the experimental results were compared with the theoretical values determined from the one-dimensional flow theory, the experimented found values were slightly below than the theoretical values. This might be because the assumptions used for gas expansion after passing the throat were isentropic.

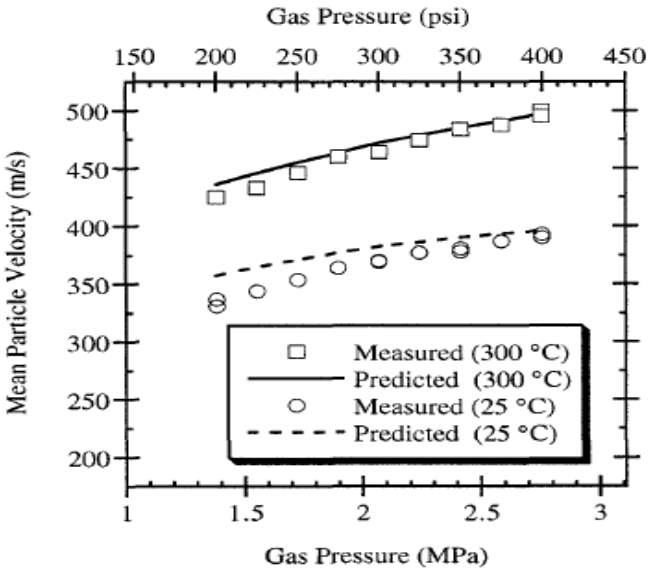

Figure 17: Effect of gas pressure on particle velocity [40]

Chang-Jiu Li *et al* [41] performed an experiment to observe the effect of operating pressure on the average velocity of the particles. Two accelerating gas pressures 1.0 and 2.6 MPa and a gas temperature maintained at 400 °C were used.

Table 6: The average particle velocity for two cases were found to be 260 and 325 m/s respectively [41]

Condition	Gas	Pressure, MPa	Temperature, °C	*k*	*n*
C5	N_2	1.0	400	1231.3	0.36
C6	N_2	2.6	400	1347.5	0.36

Cold spray systems are further subdivided into two categories high pressure systems and low pressure systems on the basis of gas pressure. A separate gas compressor is required in these systems, higher pressure gases and a gas such as helium is used in this system because of its low molecular weight to achieve very high particle velocity. In a low pressure system a powder stream is injected into the nozzle at the point where gas has expanded to low pressure. Since no

pressurized feeder is required in this system, it is often used in portable cold spray systems.

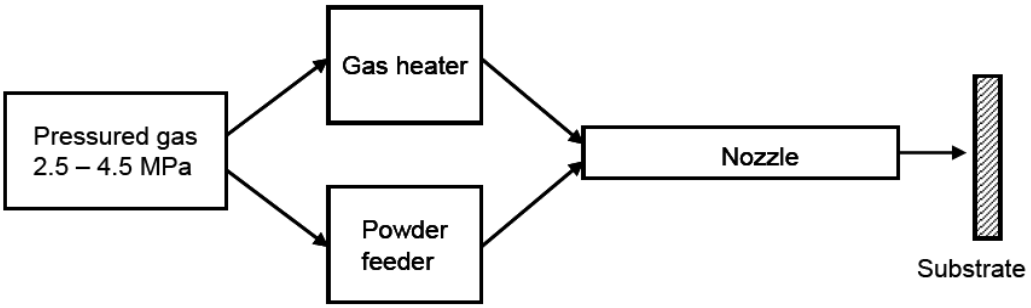

Figure 18: High pressure system [32]

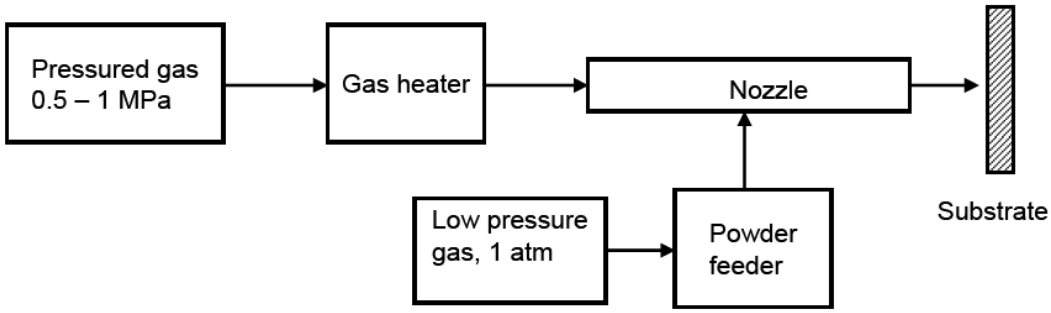

Figure 19: Low pressure system [32]

2.4.3 THE EFFECT OF THE TYPE OF GAS

In cold spray processes the type of gas used to spray powder particles plays an important role in the acceleration of particles. In most cases nitrogen, helium, air or the mixture of air and helium or air and nitrogen are used as carrier gasses because of their lower molecular weight [42].

Initially experiments using helium as a carrier gas were very successful in achieving high adhesion and corrosion resistant coatings. Cold spray process parameters were also developed with nitrogen to reduce the costs while maintaining satisfactory coating performance [43]. In one-dimensional flow

theory the mach number at the throat is assumed to be unity and the velocity of gas can be calculated from:

$$\boldsymbol{V = \sqrt{\gamma RT}}$$

γ is specific heat ratio and T is temperature of gas

where R is the specific gas constant (the universal gas constant is divided by the gas molecular weight). The above equation shows why it is often found that helium makes a better carrier gas for cold spraying. It has a smaller molecular weight and higher specific heat ratio [24]. The specific heat ratios of nitrogen and helium are 1.4 and 1.66 respectively. The specific gas constants for nitrogen and helium are 296.8 J/Kg K and 2,077 J/Kg K respectively. According to the above equation the velocity of nitrogen will be lower than the velocity of helium, and when the temperature of the gas is increased the gas velocity increases and subsequently so does the particle velocity. The drag force on particles increases because of an increase in gas pressure as a result of an increase in gas density [34].

Experiments have been undertaken to observe the efficiency of coating formation as a result of difference in the measured particle velocities with both nitrogen and helium as carrier gases. The studies have shown that of the high particle velocity from using helium results in metallic bonding of around 75% as compared to 30 to 35% when using nitrogen as a carrier gas [44]. An optical diagnostic system was used to measure the average particle velocity of 16 mm over free jet. Particle velocities were predicted using converged flow solutions.

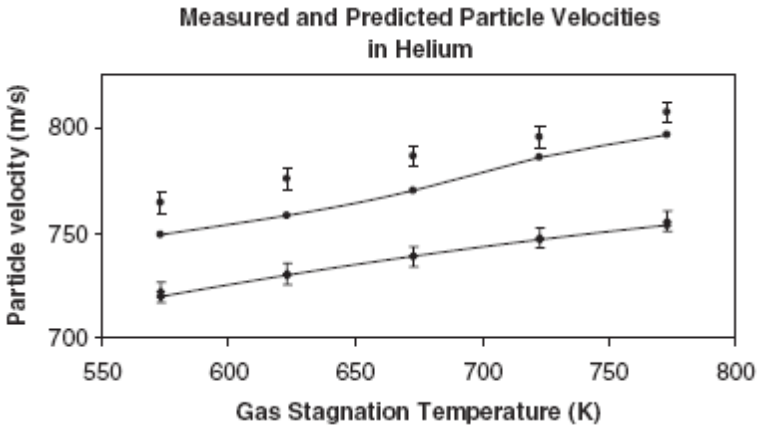

Figure 20: Comparison between measure average particle velocity and predicted average particle velocity using ●: Helium, 24 bars. ♦: Helium, 20 bars [45]

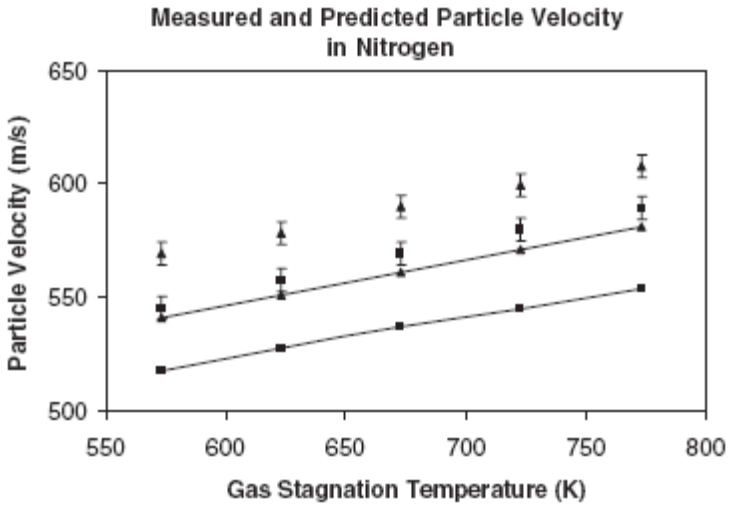

Figure 21: Comparison between measure average particle velocity and predicted average particle velocity using ▲: Nitrogen, 24 bars. ■: Nitrogen, 20 bars [45].

The above figures show that increasing the gas temperature increases the gas velocity throughout the nozzle gun, and hence more particle velocity. When the helium is used as a carrier gas it gives a higher particle velocity than nitrogen as the stagnation condition changes. It can be seen that there is an increases in

particle velocity of up to 200 m/s in the case of helium compared with nitrogen [45].

When helium and air are compared as carrier gases for spraying powder particles, then results show that at the same total gas temperature the low molecular weight, monoatomic helium has more qualities of a good carrier gas than diatomic, higher molecular weight air [46]. When calculated theoretically it is found that the particles reach 42% of the gas velocity when helium is used and 62% of the gas velocity when air is used. Since the helium velocity is 2.5 times that of air, by using helium gas a higher particle velocity is achieved [40].

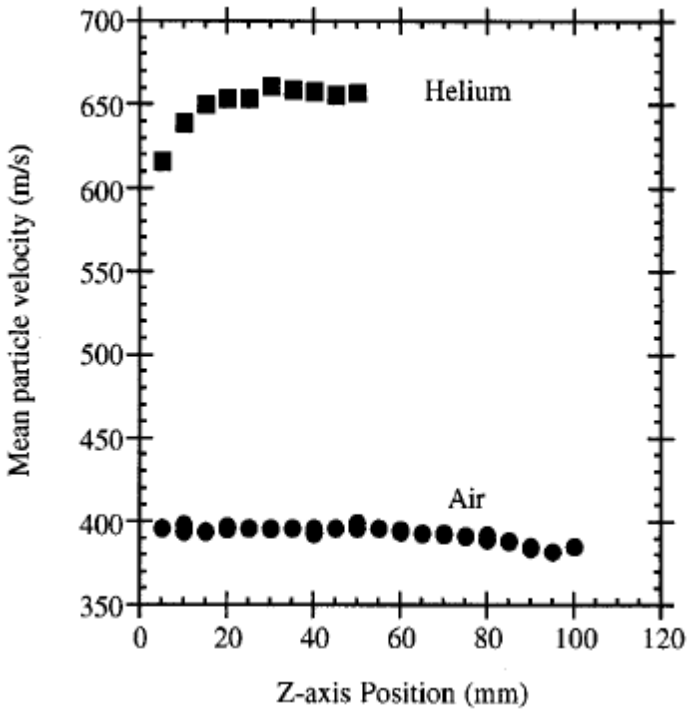

Figure 22: The mean particle velocity versus z-axis position (x = 0, y= 0). 22 µm copper particles powder; 200 °C, 2.1 MPa helium or air as driving gas [40]

2.4.4 THE EFFECT OF PARTICLE SIZE

Previous study show that the powder particles used for spraying have a wide size distribution range [47]. The powder is fed into a gas stream flowing through the nozzle. The acceleration of each particle depends upon its size. Particles cannot make a coating if they are very small in size or light in weight, because then they will follow the flow and if the powder particles are very heavy or large in size they will not get the kinetic energy from the carrier gas to strike the substrate [47]. Small particles achieve high acceleration and large particles achieve less acceleration. For making a successful powder deposit only the particles with a velocity greater than a critical velocity can contribute to the coating. Hence it is very important to consider the particle size before carrying out cold spraying. The particles size distribution can be expressed by the following Rosin-Rammler formula:

$$f_m = \left\{1 - exp\left[-\left(\frac{d_p}{d_0}\right)^m\right]\right\}.100\%$$

where d_p is the particle diameter, f_m is the cumulative mass fraction of all particles with the diameter less than d_p, d_0 and m are constants which depends on the powder used and can be found experimentally. The particle size range can be determined as follows:

$$f_m = \left\{1 - exp\left[-\left(\frac{d_p - d_{min}}{d_0}\right)^m\right]\right\}$$

$$.\left\{1 - exp\left[-\left(\frac{d_{max} - d_{min}}{d_0}\right)^m\right]\right\}^{-1}.100\%$$

where d_{max} and d_{min} are the maximum diameter and minimum diameter of the powder particles used for spraying. The following graph shows the effect of particles size on the particle velocity when nitrogen and helium are used as carrier gases.

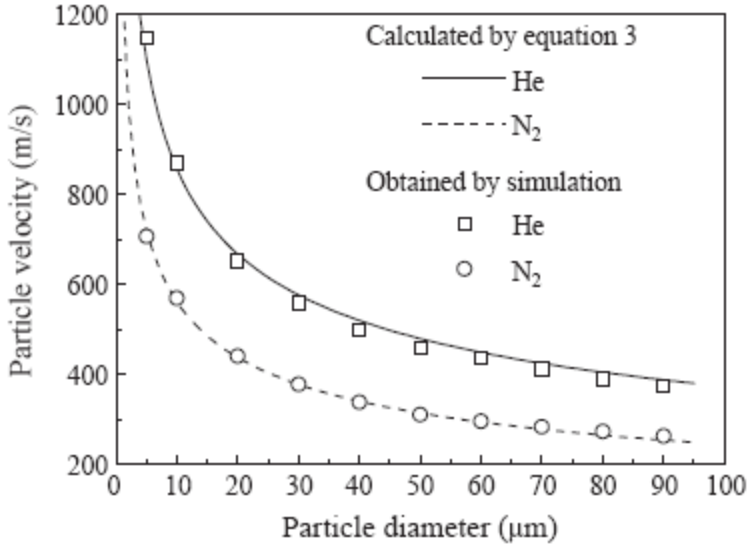

Figure 23: The effect of particle diameter on particle velocity under He and N_2 gases operated at the inlet pressure of 2 MPa and temperature of 340 °C [48]

At high temperatures more plastic deformation occurs in particles when they strike a substrate and this improves deposition efficiency [49]. A previous study shows that the particle temperature reaches maximum value when the diameter of the particle is 10μm. This behaviour is determined by the particle and gas phase heat transfer. There is a maximum temperature profile for the smaller particles because the heat transfer rate is faster for smaller particles. In larger particles, the temperature increases slowly [50].

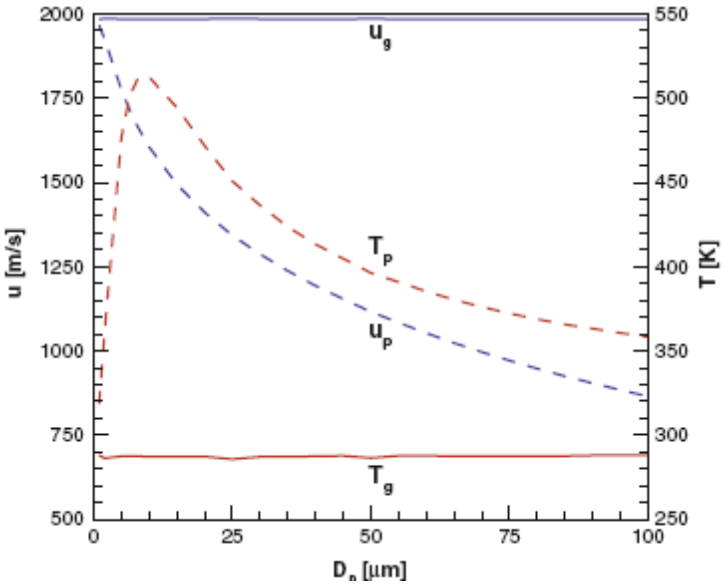

Figure 24: The influence of particle size on particle velocity and particle temperature [50]

For spraying titanium powder particles, calculations were performed by T. Marrocco *et al* [51] to determine the influence of particle size on the particle velocity along the nozzle. Fine titanium (FTi) and coarse titanium (CTi) particle diameters 28 and 47 µm were used respectively. The figure below shows the effect of the different titanium particle sizes on the velocity of the particles when helium was used at 3 MPa, and the graph is plotted showing the velocity profile along the axial direction of the nozzle using both the compressible and non compressible drag-coefficient relationship for particle acceleration. The experiment also showed that smaller particles smaller attained a higher velocity at the nozzle outlet.

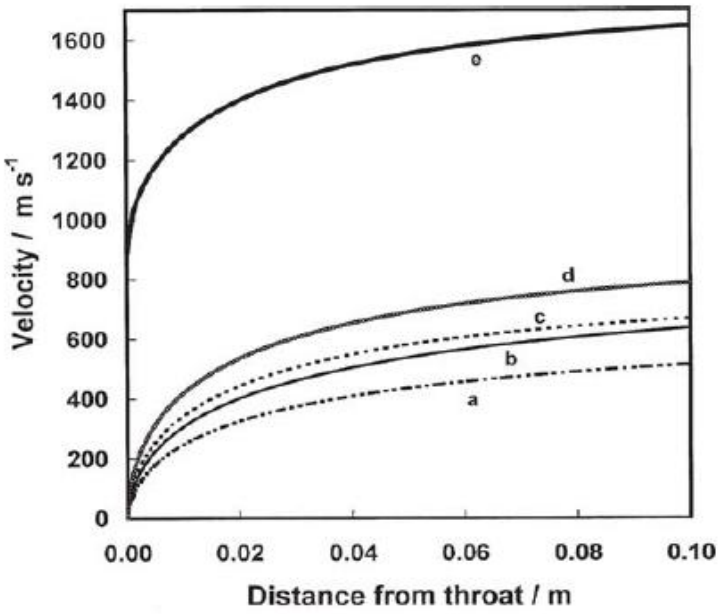

Figure 25: Velocity plot along the nozzle axis [51]

Figure 25 shows the plot of velocity versus distance along the nozzle for He gas and Ti particles (a, b) 47and 28 μm particles, respectively, using the standard noncompressible C_d relationship; (c, d) 47 and 28 μm particles, respectively, using compressible C_d relationship; (e) He gas at P_0 =29 bar and T_0 298K [51]

NOZZLE: A gas manifold to accelerate a gas to high velocity

2.5 DE-LAVAL NOZZLE

2.5.1 BACKGROUND OF THE DE-LAVAL NOZZLE

The first practical use of a convergent divergent nozzle was in the 1800s by the Swedish engineer Carl G. P. De Laval. He designed a steam turbine which incorporated a supersonic expansion nozzle upstream of the turbine blades. Initially some nozzles were convergent in shape and other designs the nozzle was nothing more than an orifice. In 1882, de Laval added a divergent section to the original convergent shape. By changing the nozzle design his steam turbines

began to run at a very high speed. Subsequently his design was demonstrated at the World Columbian Exposition in Chicago in 1893. It was through this steam turbine design that de Laval made a lasting contribution to the advancement of compressible flow [52].

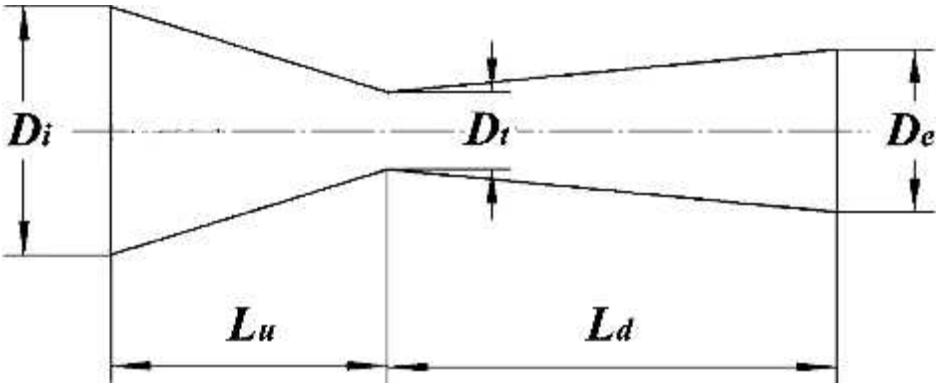

Figure 26: Diagram of de-Laval nozzle

Where: - D_t diameter of nozzle throat

D_i and De are the inlet and outlet diameter respectively

L_u and L_d are convergent and divergent lengths respectively of the nozzle

2.5.2 REASON FOR USING A DE-LAVAL NOZZLE

In cold spray, a high particle velocity can be achieved by using high propellant gas pressure and De Laval nozzle designs. Before the gas enters the converging part of the nozzle it is preheated to attain a high velocity at the throat [25].

The reason behind using the convergent divergent De Laval nozzle is to get supersonic velocity, which is possible because of its design. We can use the equation of conservation of mass to get the area velocity relation:

mass to get the area velocity relation:

$$\frac{\mathbf{d}}{\mathbf{dx}}(\boldsymbol{\rho}\mathbf{uA}) = \mathbf{0}$$

$$\boldsymbol{\rho}\mathbf{A}\frac{\mathbf{du}}{\mathbf{dx}} + \mathbf{uA}\frac{\mathbf{d}\boldsymbol{\rho}}{\mathbf{dx}} + \boldsymbol{\rho}\mathbf{u}\frac{\mathbf{dA}}{\mathbf{dx}} = \mathbf{0} \qquad (\mathbf{1})$$

A is cross section area of nozzle

$\boldsymbol{\rho}$ is density of gas and u is gas velocity

For one dimensional and steady flow of an inviscid fluid with negligible body forces, the momentum equation reduces to:

$$\frac{\boldsymbol{dp}}{\boldsymbol{dx}} + \boldsymbol{\rho u}\frac{\boldsymbol{du}}{\boldsymbol{dx}} = \mathbf{0} \qquad (\mathbf{2})$$

The process is sub-isentropic so p = p(ρ); using equation:

$$\boldsymbol{a(x,t)} = \sqrt{\left(\frac{\boldsymbol{\partial p}}{\boldsymbol{\partial \rho}}\right)}$$

We get

$$\frac{\boldsymbol{dp}}{\boldsymbol{dx}} = \left(\frac{\boldsymbol{\partial p}}{\boldsymbol{\partial \rho}}\right)\frac{\boldsymbol{d\rho}}{\boldsymbol{dx}} = \boldsymbol{a^2}\frac{\boldsymbol{\partial \rho}}{\boldsymbol{\partial x}} \qquad (\mathbf{3})$$

From equation (2) and (3), we get

$$\boldsymbol{a^2}\frac{\boldsymbol{d\rho}}{\boldsymbol{dx}} = -\boldsymbol{\rho u}\frac{\boldsymbol{du}}{\boldsymbol{dx}}$$

So that

$$\boldsymbol{Au}\frac{\boldsymbol{d\rho}}{\boldsymbol{dx}} = -\boldsymbol{A\rho}\frac{\boldsymbol{u^2}}{\boldsymbol{a^2}}\frac{\boldsymbol{du}}{\boldsymbol{dx}} = -\boldsymbol{\rho AM^2}\frac{\boldsymbol{du}}{\boldsymbol{dx}} \qquad (\mathbf{4})$$

Substituting equation (4) in equation (1), we get

$$\frac{dA}{dx} = \frac{A(M^2 - 1)}{u}\frac{du}{dx} \qquad (5)$$

Equation (5) is known as Area-Velocity relation:

Mach number: This is defined as the ratio of the fluid speed to the speed of sound. Mach number plays an important role when simulating compressible flows.

$$M = \frac{|u|}{a}$$

1. For subsonic flow i.e. M<1, we have (M^2 -1) <0. Hence if $dA/dx < 0$, then $du/dx > 0$, and if $dA/dx > 0$, then $du/dx < 0$. Thus, the velocity of a subsonic flow increases if it passes through a converging duct, and decreases as it passes through a diverging one.
2. For supersonic flow, we have (M^2-1) > 0, and the situation is reversed; when flow passes through the converging part the velocity decreases and increases when flow passes through the diverging part.
3. For sonic flow, i.e. M = 1, we have $dA/dx = 0$, which corresponds to a maximum or a minimum in the area distribution. However, only the minimum area solution is the physically realistic solution [53].

Previous studies have found that the critical velocity of most materials is more than 700 m/s, which shows the importance of supersonic flow for carrying

these particles. To optimize the nozzle shape the one-dimensional flow model has to be analytically studied knowing the given gas condition, powder size and nozzle dimensions. It is necessary to know the minimum particle velocity for designing the cold spray nozzle so that a particular powder material bonds well to a substrate. It is found that gas density and nozzle length play an important part in accelerating the particle to a velocity close to the gas velocity [54]. The graph below shows the critical velocities of different materials used for cold spraying.

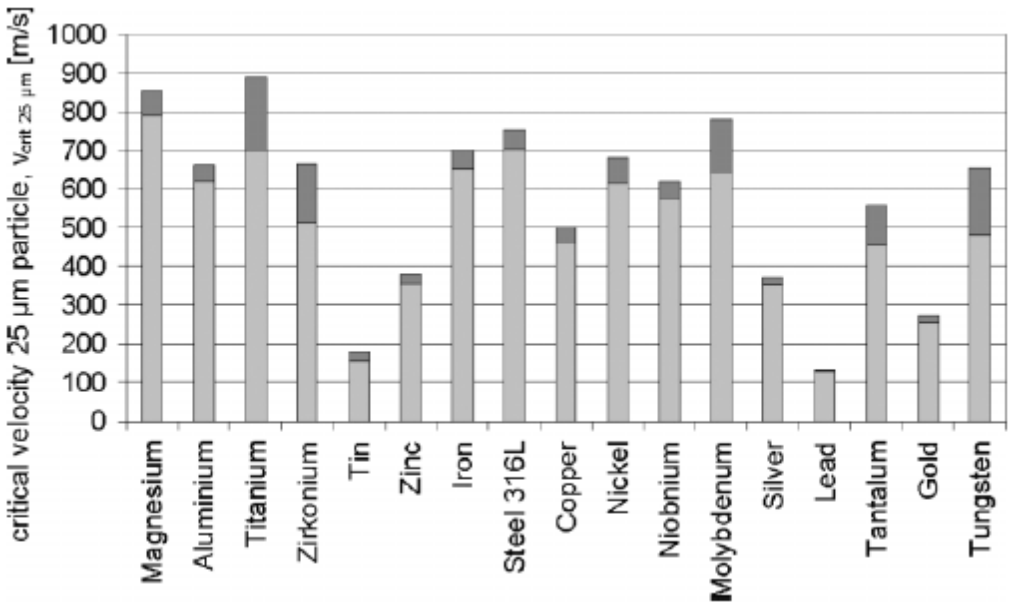

Figure 27: Calculated critical velocities for various spray materials [25]

By using computational codes like CFD the nozzle shape can be improved or evaluated. High velocity can be achieved by having a properly shaped nozzle and if the velocity is increased from the critical velocity it not only affects the deposition efficiency but also the coating quality [25].

2.6 OPTIMIZATION OF NOZZLE DESIGN

One-dimensional isentropic flow analysis has been used to show the general and specific nozzle geometry and pressure ratio required to generate a shock-free supersonic flow. B. Jodoin shows that nozzle geometry and pressure ratios are the only factors to consider when designing cold spray nozzles operating at a specific Mach nozzle. [54] By improving the nozzle design high particle velocity can be achieved which leads to high deposition efficiency. To increase the velocity of particles, gas dynamic models were used. In one of the examples it was found that if the length of the nozzle was increased from 83 mm to 211 mm, and using nitrogen as a carrier gas with 12 μm copper particles the maximum velocity can be increased from 553 m/s to 742 m/s. This is an increase in 33% in particle velocity and 80% increase in deposition efficiency [55]. The strong bond between the particle and substrate depends upon the contact pressure between the particle and substrate which is only achieved by the high kinetic energy of the particles [56][57].

From previous simulation results obtained by assuming one-dimensional isentropic flow indicates that particle velocity can be varied by changing the expansion ratio of the nozzle [34]. An optimal expansion ratio for particle acceleration of about 4 and 6.25 for nozzles with divergent lengths of 100 and 40 mm respectively were found [58]. However these optimal values may not be accurate because changes in the nozzle exit diameter in simulations were not precise. Previous studies show that nozzle inlet diameter and convergent length has very little influence on particle velocity so more attention in previous research

has been paid to the divergent length, the throat diameter and the exit diameter of the nozzle.

2.6.1 EFFECT OF THE DIVERGENT LENGTH ON THE OPTIMIZATION OF THE NOZZLE EXIT

It is found from the literature that maximum particle velocity is achieved when the divergent length is increased from 150 mm to 200 mm. By further increasing the divergent length, particle velocity changes slowly. When divergent length increases from 67.6 to 170 mm the velocity increment is 80 m/s and optimal exit diameter also increases from 5.0 to 6.2 mm [59].

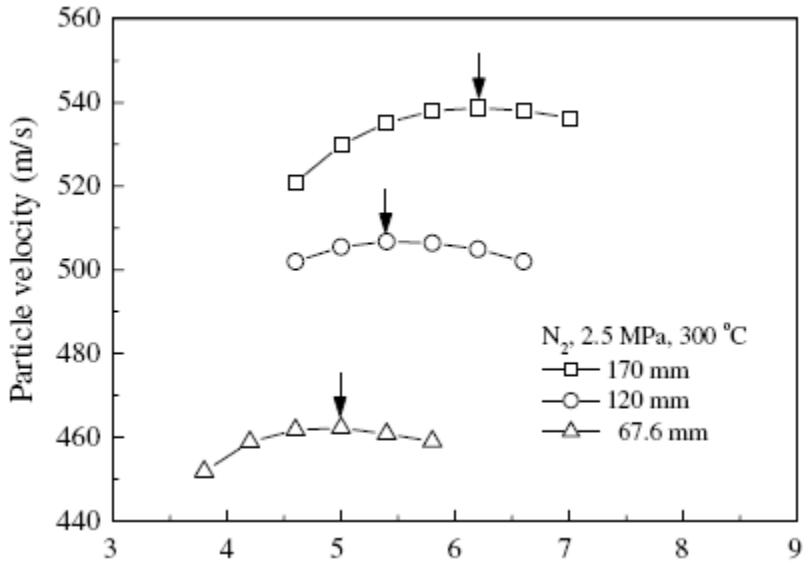

Figure 28: Effect of divergent length on optimal nozzle exit diameter [59]

2.6.2 OPTIMIZATION OF THE NOZZLE EXIT DIAMETER

The nozzle exit diameter has a significant effect on particle velocity. The effect of the exit diameter of the nozzle on different particle sizes using nitrogen as a carrier gas at a pressure of 2 MPa is shown in the figure below for a temperature

of 300 °C. The optimal diameter of nozzle exit for maximum particle acceleration is 5 mm under given conditions.

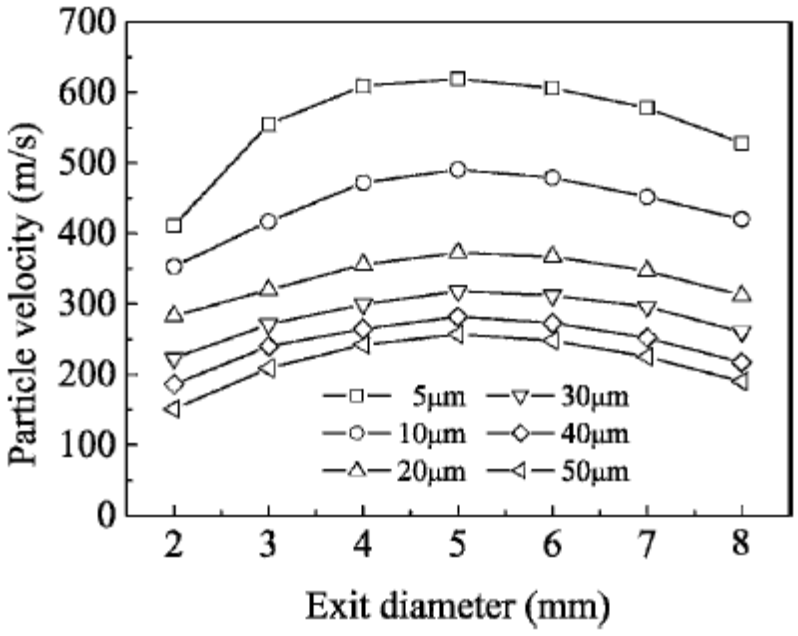

Figure 29: Effect of nozzle exit diameter on the velocity of particles with different sizes using nitrogen at pressure 2 MPa and temperature 300 °C [34]

2.7 SIMULATION OF COLD SPRAY PROCESS

Modelling and simulation are used by different research groups across the world to investigate cold spray nozzles. The isentropic flow model is used to verify the results of the simulations to cross check the results theoretically. Different simulation packages are being used like the CTH computer code which simulates the impact of particle on the substrate [56], FEM which simulates the deformation kinetics and impact pressure in a cold spray process [59], and ANSYS FLUENT software package which simulates the nozzle design and all the parameters involved in the process of loading the particles in a gas stream and coating the substrate. [60] For starting the simulation it is important to know the critical

velocity of the particles to be sprayed in order to optimize the other parameters of the spraying. The method used for detecting the critical velocity of particles involves the counting of the times the particles rebound from the substrate and using imaging technique to improve the accuracy of the measurements of small particles. [61] The critical velocities of different particles are as follows copper 500 m/s, aluminium 640 m/s, titanium 890 m/s, gold 250 m/s etc [25]. Deposition efficiency can be measured by weighing the substrate before and after the coating relative to the mass flow through the nozzle [62].

For the numerical simulation of a nozzle, a commercial software package FLUENT (Fluent Inc. Lebanon, NH) has been used to predict the flow field of the carrier gas inside and nozzle and outside before striking the substrate and the acceleration of the particles flowing in a gas stream. The main parameters involved in simulation are nozzle geometry, gas conditions [63] [58] and properties of powder particles. A de-Laval nozzle, with the main parameters of convergent length, divergent length, throat diameter, and exit diameter is used for simulation [34]. While solving compressible flow, there are gas density changes with changes in the cross-sectional area of a duct so ideal gas laws have to be used, which adds another variable, temperature T, to the calculations. Hence, the energy equation must be solved along with other equations of compressible flows. These are the initial processing conditions of process in the FLUENT software. The boundary conditions are used to specify the stagnation pressure and stagnation temperature of the carrier gas at the nozzle inlet [64].

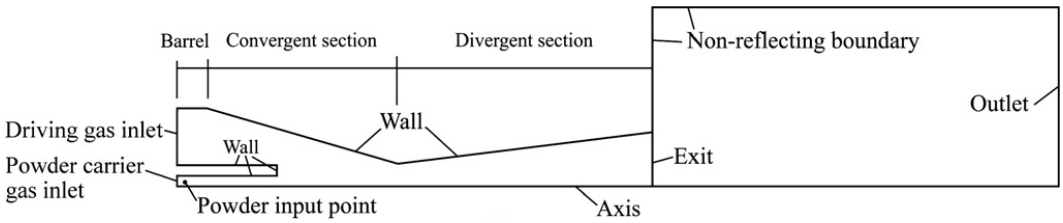

Figure 30: Typical model of nozzle used in simulations [58]

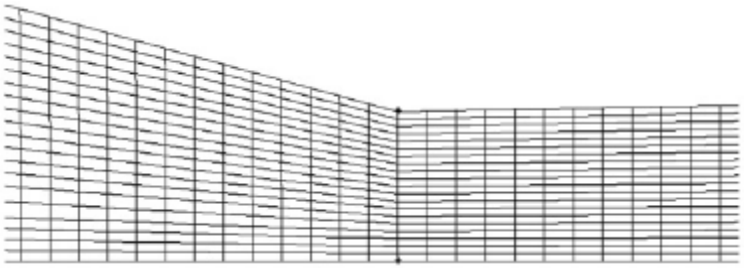

Figure 31: Example of mesh used for simulations [58]

Due to the compressible nature of flow the pressure, temperature and density of the fluid keeps on changing. According to previous studies the k-ε turbulence model which has been used to solve for the resulting turbulence in the governing gas flow equations, are given by the two-dimensional axisymetric, time dependent Navier-Strokes equation [65][66].

Previous studies show that different nozzle designs are simulated according to the type of coating required, powder particles to be sprayed and the velocity and deposition efficiency required.

3 EXPERIMENTAL PROCEDURE

3.1 INTRODUCTION TO CFD

The physical properties of all fluid flow are governed by the following three fundamentals:

1) Mass is conserved

Mass conservation equation:

$$\frac{\partial \rho}{\partial t} + \frac{\partial}{\partial x_i}(\rho u_i) = S_m$$

here S_m is the added mass, ρ is density

2) F = ma (Newton's second law)

Momentum conservation equation

$$\frac{\partial}{\partial t}(\rho u_i) + \frac{\partial}{\partial x_j}(\rho u_i u_j) = -\frac{\partial p}{\partial x_i} + \frac{\partial \tau_{ij}}{\partial x_j} + \rho_{gi} + F_i$$

Here p is static pressure, τ_{ij} is the stress tensor, ρ_{gi} is the gravitational body force (buoyancy) and F_i is the external body force. As we are dealing with supersonic flow, ρ_{gi} is zero compared to external body forces.

3) Energy is conserved

$$\frac{\partial}{\partial t}(\rho E) + \frac{\partial}{\partial x_i}(u_i(\rho E + p)) = \frac{\partial}{\partial x_i}\left[k\frac{\partial T}{\partial x_i} - \sum_j h_j J_j + u_j \tau_{ij}\right] + S_h$$

Here E is the total energy per unit mass, k is the conductivity, $\boldsymbol{J_j}$ is the diffusion flux of species j and $\boldsymbol{S_h}$ is the source term which refers to any heat source.

These basic principles for a flowing fluid can be written mathematically in the form of partial differential equations. Basically Computational Fluid Dynamics (CFD) replaces the governing differential equations with numbers to represent the fluid flow, and these numbers are put in three-dimensional space with a time interval to get the desired flow field in numerical form. The final outcome of the CFD is a group of numbers in closed form which represent a flow field analytically. CFD solutions generally require the repetitive manipulation of hundreds, or even more than millions, of tasks which are impossible for humans to do without the help of computers. The new generation computers continue to play an important role in the growth of Computational Fluid Dynamics. The application of CFD for more complex and sophisticated cases depends mostly upon the computational resources like storage capacity and computational speed (RAM) [67].

3.1.1 REASON FOR USING CFD

CFD is a simulation technique which does mechanics computationally. These days simulation has become an important tool in the field of engineering and physics and is used in applications like reconstruction and analysis of the behaviour of the engineering products or physical situations under measured boundary conditions (initial states, geometry, loads, etc.) The reasons for using CFD are:-

a) A need to forecast performance: Companies need to be able to predict the behaviour and performance of their new product to determine and reduce flaws which could affect their market value e.g. aircraft and car manufacturers. Developing a new product is very expensive (about $\$4.10^9$ for a new aircraft, $\$10^9$ for a new car; these and all subsequent quotations are in 2000 US$) [68]. In this case the CFD simulation can help to predict the behaviour and provide important information.

b) Cost of experiments: CFD can help to reduce the cost of experiments related to fluid dynamics. Performing an experiment in large wind tunnels costs more than $\$10^5$, excluding the labour costs, modelling, result analysis, and other hidden costs and time loss in designing.

c) Impossibility of experiments: In some cases it is impossible to perform the experiments for example experiments related to atmosphere, space, nuclear explosion, and some medical experiments which cannot be performed on patients.

d) Insight: CFD simulation gives more information than an experiment would, for example, a grid consisting of 2.10^7 cells is equivalent to 2.10^7 numbers of measuring instruments. No equipment could have this many measuring locations.

e) Computer speed and memory: The speed of computers and their storage capacity almost double every one and half years (Moore's law). Simulation therefore gives more correct solutions as the algorithms

currently under development which increases the accuracy and speed of calculations [68].

3.2 INTRODUCTION TO FLUENT

Fluent is the world's largest provider of commercial computational fluid dynamics (CFD) software and services. For doing Computational Fluid Dynamics FLUENT uses computer as a tool for analysing and designing models. Fluent is computer software used for making models of flowing fluid and heat transfer. In fluent geometry of very complex models can be formed by using different type of meshes for solving the problems related to fluid flow. It also allows the mesh refining or coarsening depends on the solution required [69].

Fluent is formed by the C language of computer and has used full freedom and functions provided by the language. By using powerful computers FLUENT can run separately simultaneous processes on different CPUs connected in series or parallel having same desktop. Through an interactive, menu drive interface all the functions needed to compute a solution and display the results are accessible in Fluent [69].

FLUENT PACKAGE INCLUDES THE FOLLOWING PRODUCTS:

I. FLUENT, the solver.

II. GAMBIT, for pre-processing of geometry modelling and generating grid.

III. TGrid, an additional pre-processor for generating volume grids from existing boundary grids.

IV. Filters (translators) for importing surface and volume grids from CAD/CAE packages such as ANSYS, CGNS, I-deas, NASTRAN, and others [69].

Gambit is used for making a grid and geometric model and Tgrid is used to generate a variety of grids from an existing mesh boundary (generated by Gambit or CAD/CAE package). Fluent performs all the operations after reading the grid. The process starts with specifying boundary conditions, setting fluid properties, processing the solution, modifying the grid and analysing the results [69].

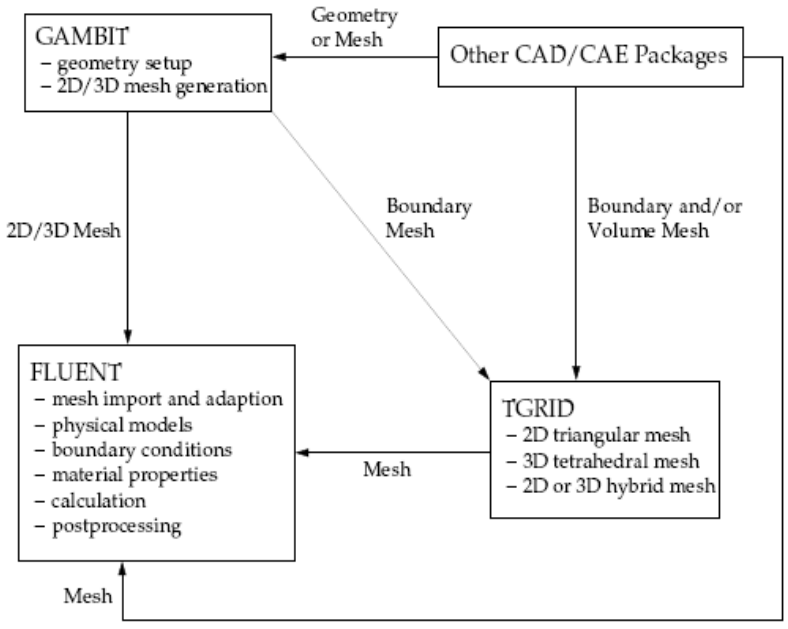

Figure 32: Flow chart of simulation in FLUENT

3.2.1 CFD VALIDATION

It is important to validate the computational values before implementing them into the practical work and assessing their usefulness. Validation is also called ‘solving the right equations’. It is usually done by comparing the computational values with those from previous experimental data to see whether the computational simulation agrees with the real world observations. In the case of examining the velocity of titanium particles through the nozzle, validation will be done by comparing the simulation results with previous experimental results of cold spraying. Different applications require a different degree of accuracy in the validation, so the validation process is flexible to allow for different degree of accuracy.

3.3 MODEL GENERATION OF NOZZLE IN GAMBIT

The first step to starting a simulation using the commercial computational code Fluent is to model the geometry either by using any CAD software package or by using the T-Grid or Gambit of the Ansys package. To solve a problem using Fluent first, the grid is generated in Gambit. Next the boundary conditions or flow parameters are defined. These represent the model in the software and determine the results obtained. The mesh enables Fluent to create a flow field through which a pressure, velocity and temperature profile can be generated.

1. COMPUTATIONAL DOMAIN: This is formed by generating the grid (mesh) which consists of small cells. These small cells form the whole domain area for a two-dimensional model. The output of the CFD highly

depends upon the quality of the mesh, so the initial step to getting good results is making a good quality mesh.

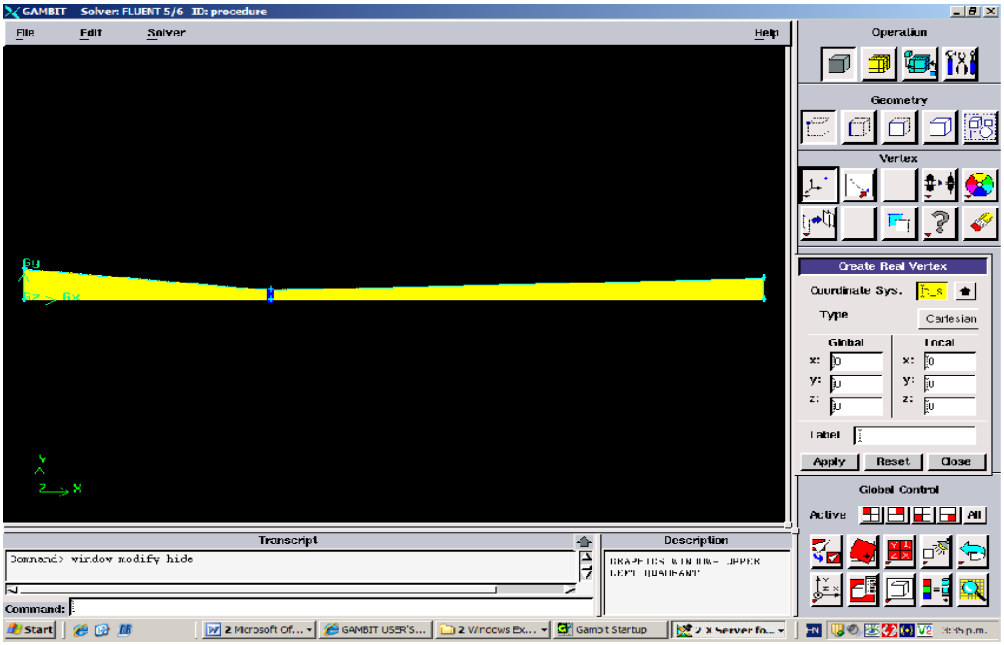

Figure 33: User interface of GAMBIT

2. BOUNDARY CONDITIONS: These are specified on the edges of the two-dimensional model to define boundaries such as pressure inlet, pressure outlet, walls, axis, symmetry, and mass flow inlet. Setting boundary conditions helps the software to read where the flow is coming from and where the flow is going to, and what walls bound the flow in a certain area.

3. DOMAIN TYPE: It is required to specify the domain type either as solid or fluid before generating the mesh, so that we can select the common fluid or solid from the material database in Fluent and define properties such as density, specific heat, thermal conductivity and molecular weight for CFD simulation.

3.4 EXPERIMENTAL PROCEDURE

To attain the supersonic velocity of the gas stream it is necessary in this case to construct the geometry of the convergent divergent de-Laval nozzle model [70]. Gambit is used to generate the mesh to create the flow field to give the pressure and temperature profile in the nozzle. The simulation gives the various properties of the flowing fluid and how different parameters affects the outlet velocity of the titanium particles and to know the optimum parameters for spraying titanium particles during cold spraying. The dimensions of the convergent-divergent nozzle are:

Table 7: Dimensions of nozzle used for modelling

Inlet diameter	6 mm
Convergent length	20 mm
Throat diameter	2 mm
Divergent length	40 mm
Outlet diameter	4.114 mm

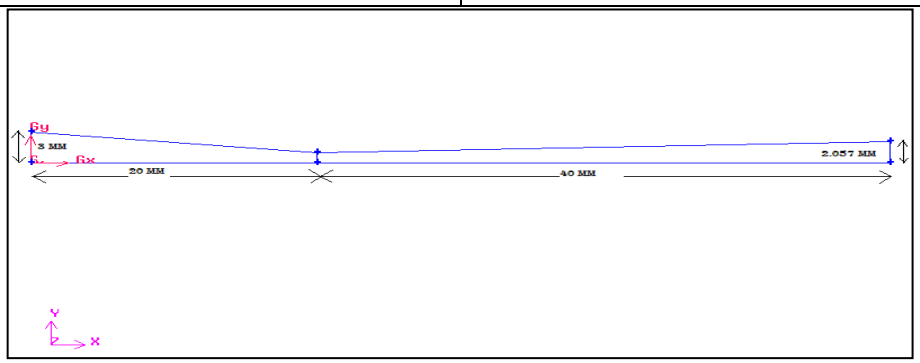

Figure 34: Model of axisymmetric nozzle drawn in GAMBIT

An axisymmetric model of the nozzle was used in the simulation. The model of the nozzle as shown in figure above was half of the nozzle from the centre axis of the nozzle. The reasons for making it axisymmetric were:

- It reduced the computational effort required to solve the problem, Fluent took less time to solve the problem and create the flow field.
- Flow field and geometry were symmetrical
- Zero normal velocity at the plane of symmetry
- Zero normal gradients of all variables at plane of symmetry
- No input required

The plane of symmetry was specified as the axis in boundary specifications and the nozzle model was defined such that flow, pressure gradient and temperature were zero along this specified edge of the domain.

Using an axisymmetric model reduces computational effort but it does not affect the outcome of the simulation. Y. Li *et al*., who investigated both the axisymmetric nozzle and two-dimensional full nozzle, found good agreement with the experimental results [71].

3.4.1 MESH GENERATION

A "Bottom-up" approach was used to generate the model mesh. First vertices were created using a grid system, and than the edges were created by joining the vertices together. The face was created by joining the edges together. The mesh created for the nozzle was a single block, structured mesh. The nozzle inlet was divided into 100 nodes, consisting of a convergent part 20 mm long divided into

200 nodes and a divergent part 40 mm long divided into 300 nodes. The total number of cells constituting the mesh was 50,000. Mesh independence was also studied to see the effect of mesh resolution on the outcome of the simulation by using a mesh with a different number of cells. The number of cells in the different meshes was 11,00, 13,650, 18,900, 50,000, 88,000 for the nozzle geometry.

Table 8: Different mesh sizes for the computational domain

No.	Number of cells	Outlet velocity (m/s)
1.	11,000	611.133
2.	13,650	611.456
3.	18,900	611.607
4.	50,000	612.11
5.	88,000	612.890

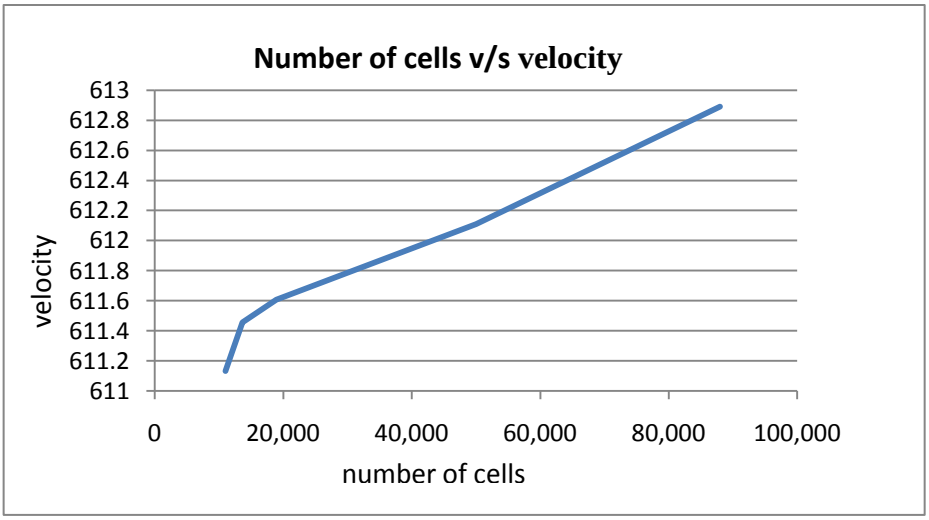

Figure 35: The outlet velocity of the nozzle using different mesh resolutions

It was evident from the results that the different meshes (number of cells) did not make much difference to the velocity of the gas stream at the outlet. It was decided that a mesh with 50,000 cells would be used because a mesh with 88,000 cells was taking double the computational time of 50,000 cells with not much difference in velocity profile.

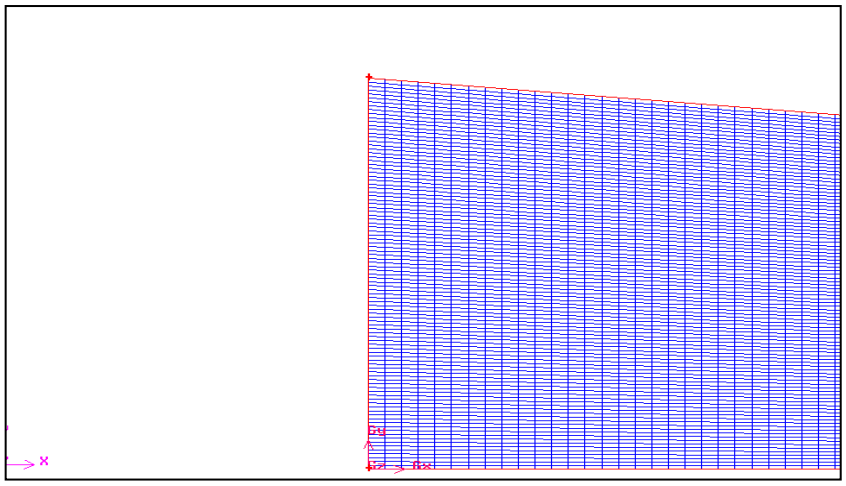

Figure 36: Sample of the mesh of the inlet of the nozzle

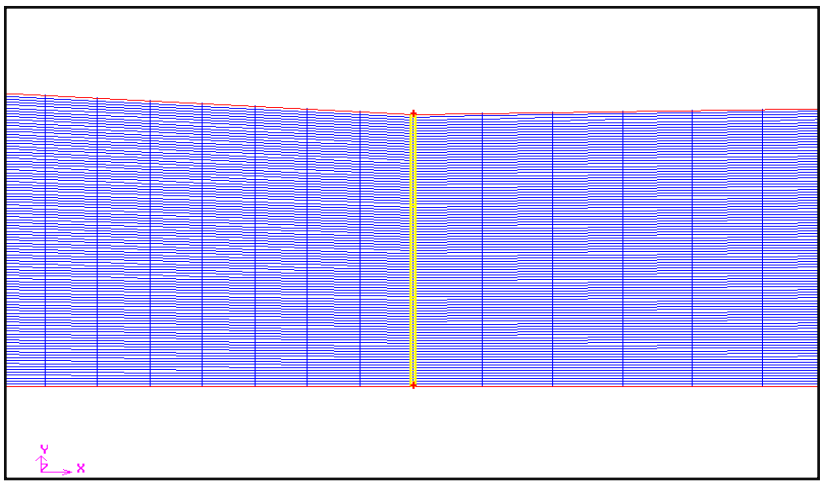

Figure 37: Sample of mesh of the throat of the nozzle

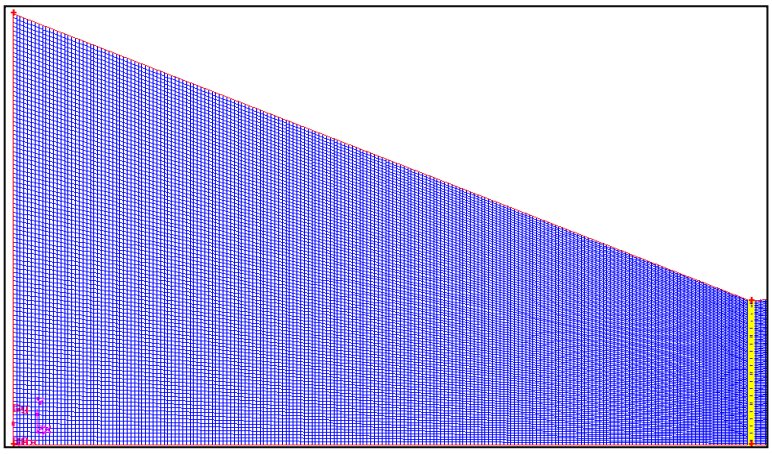

Figure 38: Sample of the mesh quality

3.5 COMPUTATIONAL RESOURCES AND TIME

The systems uses Pentium(R) 4 CPU 3.80 GHz processors and 4 GB RAM which were used for the calculations. The calculations were executed on the 5 systems connected in series on a single processor which was connected to a supercomputer CPU. The operating system was windows XP professional based.

The computational time for simulation of supersonic flow through a nozzle was between 13 to 16 hrs of CPU time depending upon the type of gas used, pressure and temperature. As the density of the helium gas is small and high gas velocity is involved in its simulation the computational time for a simulation of helium was more than for air and nitrogen. The calculations were done for different gas temperatures and different gas pressures to see their effect on the outlet velocity. The total computational time taken for all simulations was 1125 hrs CPU time approx.

3.6 MODEL PARAMETERS

The nozzle for cold spraying of titanium particles was simulated by commercial code FLUENT 12 using the 2D double precision density solver to see the effects of the different parameters on the velocity of the titanium particles, and how changing different parameters like temperature, pressure and size of the titanium particles affects their velocity. From the literature, it was found that the velocity of the particles could be influenced by the nozzle expansion ratio (i.e. ratio of area of exit of nozzle to the area of throat). The nozzle used for calculations had an expansion ratio of 4.11 which is in the range of expansion ratios specified by Wen –Ya Li *et al* [34].

The coupled implicit density-based solver along with the Least Square Cell Based gradient method was used to simulate the flow field inside the nozzle. The flow, turbulent kinetic energy, and turbulent dissipation rate were modelled using second order upwind accuracy.

3.6.1 SECOND ORDER SCHEME

In the second order scheme, the values of cells are computed by using a multidimensional linear reconstruction approach. This approach was used for obtaining higher order accuracy and is achieved at cell faces by a Taylor series expansion of the cell centred solution of the cell centroid. The face value $\emptyset_f$ is computed using the following expression:

$$\emptyset_f = \emptyset + \nabla\emptyset.\Delta s$$

where $\emptyset$ and $\nabla\emptyset$ are the cell centred values and their gradient in the upstream cell, and Δs is the displacement vector from the upstream cell centroid to the face centroid. This formulation requires the determination of the gradient $\nabla\emptyset$ in each cell. This gradient is computed by using the divergence theorem, which in discrete form is written as:

$$\nabla\emptyset = \frac{1}{V}\sum_{f}^{N_{faces}} \emptyset_f A$$

Here the face values $\emptyset_f$ are computed by averaging $\emptyset$ from the two cells adjacent to the face. Finally, the gradient $\nabla\emptyset$ is limited so that no new maxima or minima are introduced.

3.7 TURBULENCE MODELLING

The fluid flowing through the nozzle had a very high Reynolds number (more than 50,000), so the flow can be said to be fully turbulent. This met the requirement of a numerical turbulent model for modelling the flow of titanium particles through the nozzle in the gas jet. Different turbulence models adopt different approaches for tackling turbulence but choosing the right model ensures the accuracy of the final solution. Modelling turbulence is very complex and a highly technical field, and the selection of a turbulence model depends on factors including accuracy required, computational time, resources available, and application.

In the last few years, turbulence models based upon Reynolds-averaged Navier-Strokes (RANS) equations have been used for industrial applications because of their low-cost and reasonable accuracy for different types of flows [72]. A K-ε

model is commonly used for modelling turbulence and is an industrial standard for modelling flow in CFD because of its versatile nature and robustness. It is also found from the literature that the K-ε model gives a fairly accurate prediction of the turbulence in the flow of metal particles through the gas stream flowing through the convergent-divergent nozzle [34][65][73][41][74]. A further reason it was chosen is because it is computationally efficient. This method was developed in 1974 and was the first to propose the two basic equations in computational fluid dynamics [75].The assumptions made for the formulation of the model were as follows:

a) Isentropic conditions
b) The flow is axisymmetric
c) Steady state

K-ε is a two equation model which means it has two transport equations to represent the turbulent nature of the flow. The first transported variable is turbulence kinetic energy K, which calculates the energy in the turbulence, and the second transported variable is the turbulence dissipation ε, which calculates the scale of the turbulence. The eddy viscosity for the K-ε model is typically derived from:

$$\boldsymbol{\mu_T = C_\mu \rho \frac{k^2}{\varepsilon}}$$

where $\boldsymbol{C_\mu}$ is a model coefficient

Reynolds-average Navier-Strokes equations were used to describe the flow field and the Boussinesq assumption was used. As a result the standard K-ε model was

used to account for the effect of turbulence in the flow field. The standard K-ε model was used for the simulation to account for the turbulence and simulation of titanium particles. This model deals with the free shear layers in a proper way and the method is validated as it was used by K. Pougatch *et al.* [76] for gas-liquid modelling in the De-Laval nozzle, K. Taylor *et al*. [77] for simulating particles, T. Han *et al*. [31] for modelling powder injection, Wen-Ya *et al*. [34] for designing nozzle and Wen-Ya Li *et al*. [58] for nozzle design optimisation. It was concluded that this turbulence model was appropriate for this application because of its solution accuracy and relevance.

3.8 BOUNDARY AND INITIAL CONDITIONS

As shown in the figures below, the boundary types were specified in GAMBIT, which defined the model parameters such as from which direction flow is coming, in which direction it is leaving and which boundaries of the domain are adiabatic.

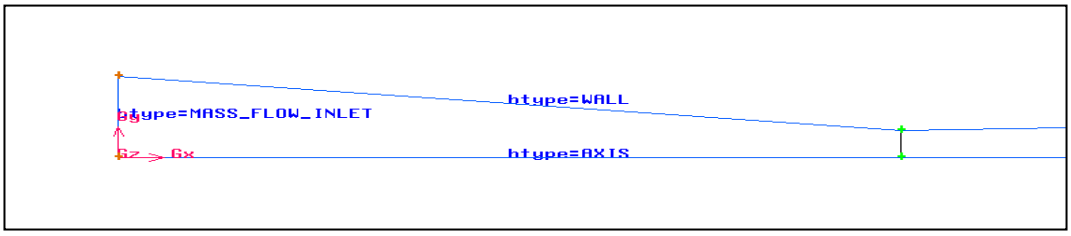

Figure 39: Boundary type of the converging part of nozzle

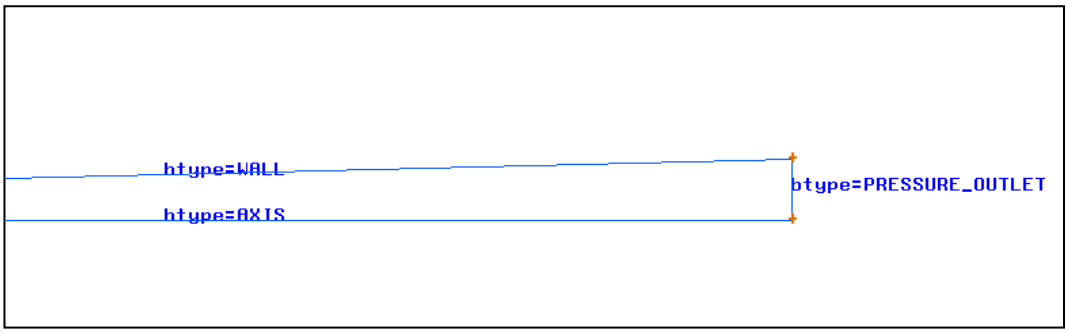

Figure 40: Boundary type of the diverging part of the nozzle

3.8.1 FLOW FIELD

For the nozzle domain, mass flow inlet was used as the boundary condition at the nozzle inlet because of the better convergence rate compared to the pressure inlet [70]. The inlet pressure for cold spraying was ranged from 1.5 MPa to 3 MPa, and the Mach number at the throat was assumed to be unity. By using the isentropic flow equations, the mass flow rate was calculated as 0.0438 Kg/sec. The pressure 1.5 MPa was produced upstream of the nozzle as a result of this mass flow rate. The velocity of flow at the inlet was zero so static pressure and total pressure were equal, and total temperature and static temperature were equal. The total temperature at the inlet boundary condition was 300 K. The direction of the velocity vector was assumed to be normal to the direction of the boundary (outlet). The value of turbulence intensity was set at 1% and the length scale was 20% of the nozzle inlet diameter. These values were validated by the cases in which these values were used for similar kinds of simulation or making flow fields [70][78][79]. Standard K-ε corrects these turbulence values according to the turbulence produced in the flow [31]. In order to achieve maximum velocity and to see the effect of changing parameters, like pressure and temperature, on the gas outlet velocity, air, nitrogen and helium were used to simulate the supersonic flow

through a convergent-divergent nozzle. The table below shows the different mass flow rates used for air, nitrogen and helium for exerting pressures ranging from 1.5 MPa to 3.1 MPa:

Table 9: Table of mass flow rate (kg/sec) of air, nitrogen and helium at 300 K

Pressure at inlet (KPa)	Air (Kg/sec)	Nitrogen (Kg/sec)	Helium (Kg/sec)
1500	0.0438	0.0413	0.016
1900	0.053	0.0523	0.0206
2300	0.0643	0.0633	0.025
2700	0.0754	0.0743	0.0293
3100	0.0866	0.0853	0.0337

The temperature of the gas for the inlet boundary condition was gradually increased from 300 K to 700 K. The mass flow rate of the gas depends upon the temperature at the throat which changed when the temperature was changed at the inlet boundary condition.

Pressure outlet was selected as the boundary condition at the nozzle outlet, with the static pressure equal to ambient pressure. Neighbouring cells were selected to obtain the direction of the velocity vector. The nozzle walls were considered to be adiabatic. As the heat transfer from the walls to the surrounding ambient was negligible the temperature of the walls was assumed to be 300 K.

3.8.2 FLUID PROPERTIES

Compressible fluids are those in which the fluid density changes with the high pressure gradients. For gases, varying the temperature changes the gas density. The fluid properties were changed from default settings to account for compressibility, and for changes in thermophysical properties like density with temperature. The ideal gas law was selected in the density drop-down list. The ideal gas law for compressible flows is:

$$\boldsymbol{\rho = \frac{p_{op} + p}{RT}}$$

where, p is the local gauge pressure predicted by FLUENT

$\boldsymbol{p_{op}}$ is the operating pressure

For ideal gases, the dynamic viscosity μ is related to the absolute temperature T. Sutherland's law was used to account for the change in viscosity with changing temperature. Sutherland's law was selected as it is suitable for simulating high-speed compressible flows [80]. It gives quite accurate results with minimum errors over a wide range of temperatures [81]. Sutherland's law can be expressed as:

$$\boldsymbol{\mu = \mu_{ref} \left(\frac{T}{T_{ref}} \right)^{3/2} \frac{T_{ref} + S}{T + S}}$$

where, $\boldsymbol{T_{ref}}$ is reference temperature

$\boldsymbol{\mu_{ref}}$ is the viscosity at the $\boldsymbol{T_{ref}}$ reference temperature

S is the Sutherland temperature

3.8.3 DISCRETE PHASE MODELLING

The cold spray process does not only deal with gas conditions, the most important parameter is the spray particle velocity. Discrete phase modelling (DPM) in FLUENT was used to examine the acceleration of the particles inside the nozzle domain. The discrete phase model option solves the equation of motion for discrete phases dispersed in the continuous phase, by adopting a Lagrangian frame of coordinates which leads to the computation of the particle trajectories [79]. DPM helped to determine the influence of the size of the titanium particles on their acceleration at the nozzle exit. Titanium particles ranging from 5 μm to 50 μm were used in the simulation to see their effect on the outlet velocity. Spherically shaped titanium particles were used with an initial velocity of 100 m/s and an initial temperature of 300 K. The powder mass flow rate used for particle tracking was 10-15% less than the gas mass flow rate so that it would not disturb the gas flow field.

3.9 ASSUMPTIONS

The following assumptions were made for DPM:

1. The titanium particles were spherical in shape
2. The particles travelled in the axial direction of the nozzle
3. The interaction between titanium particles was negligible
4. The particles were accelerated by the drag force of the gas used
5. The temperature inside the titanium particle was uniform

3.10CONVERGENCE ASSESMENT

A solution is said to be converged when the rate of change of the residuals approaches zero. This simulation solution was considered to be converged when the residuals for energy, continuity, x, y velocities, turbulence kinetic energy k, and turbulence dissipation rate ε all fell below $1x10^{-4}$. The solution was considered converged when the mass balance error was less than 0.2% of the net flow through the nozzle domain.

In some cases the convergence criterion was used as a compromise between the processing time and accuracy of solution. The convergence history of the static pressure was also used for judging the convergence, when the static pressure at the nozzle outlet was not changing with the number of iterations the solution was considered to be converged.

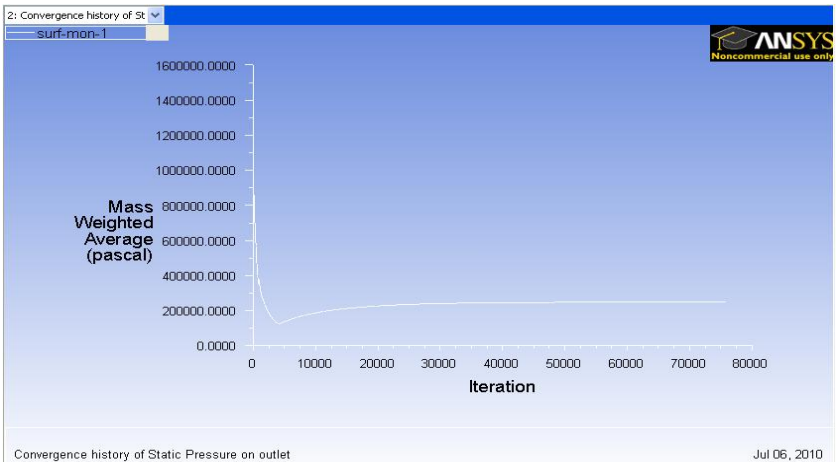

Figure 41: Plot of convergence monitor in FLUENT

4 RESULTS AND DISCUSSIONS

In this section the results of a simulation of gas flow inside the nozzle and the affect of different parameters on the velocity of titanium particles are presented:

4.1 FLOW OF CARRIER GAS INSIDE THE NOZZLE

For creating a flow field inside the nozzle air, nitrogen and helium were used as carrier gas**es**. Pressure, temperature, velocity and density profiles were generated for gas pressure**s** ranging from 1.5 MPa to 3.1 MPa and inlet gas temperature ranging from 300 K to 700 K. Different profiles obtained after simulation showed that most of the changes in the variables**:** pressure, temperature, velocity and density were near the throat of the nozzle. A **v**elocity profile for air, nitrogen and helium at an applied gas pressure of 1.5 MPa and stagnation temperature of 600 K are shown below:

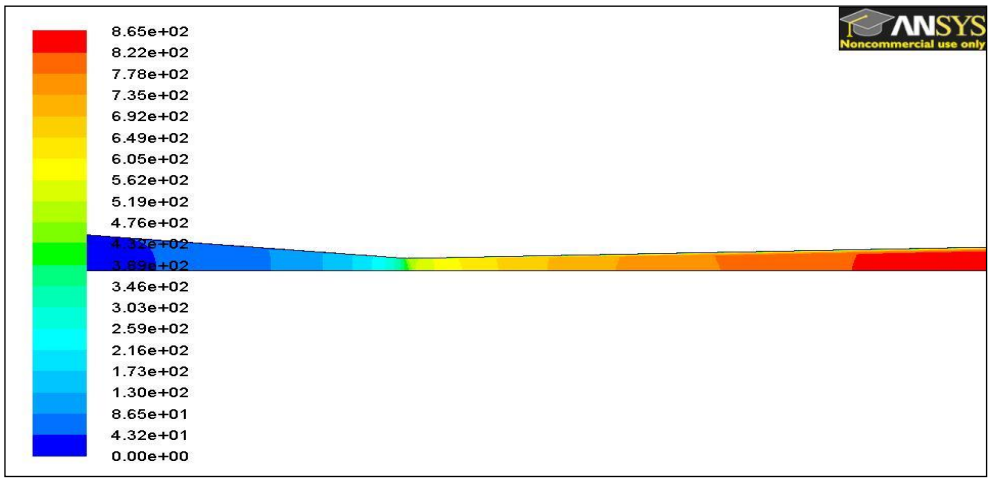

Figure 42: Velocity contour plot using air as carrier gas

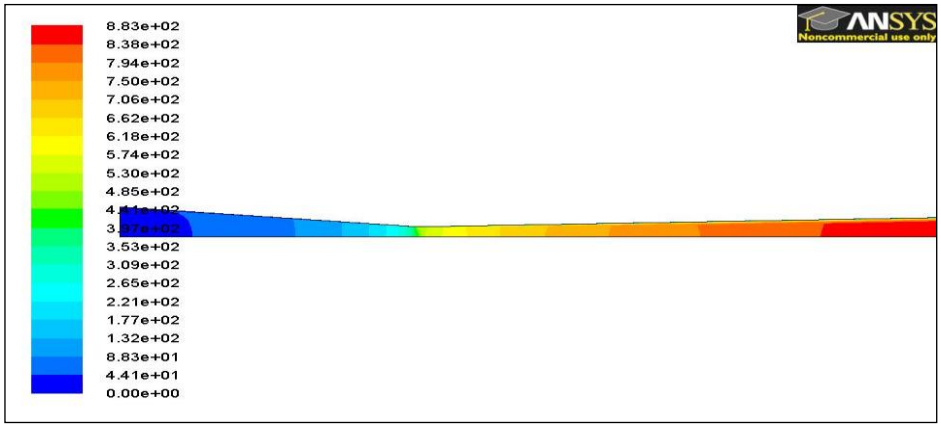

Figure 43: Velocity contour plot using nitrogen as carrier gas

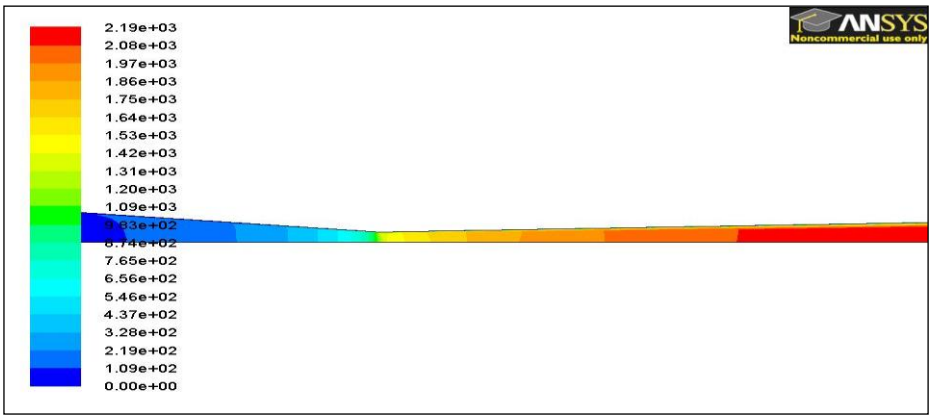

Figure 44: Velocity contour plot using helium as carrier gas

The velocity contours with different carrier gases shows a different velocity at the nozzle exit**:** 864.79 m/s, 882.53 m/s and 2185.45 m/s for air, nitrogen and helium respectively. Similar profiles were obtained for other flow parameters too at different gas pressure and temperature and using different nozzle dimensions. As shown in the figure below**,** the pressure profile for air at an applied pressure of 1.5 MPa and temperature of 600 K, with a decrease in static pressure towards the exit of the nozzle**,** the Mach number of air increases as shown in Fig 43 according to the gas dynamic equation:

This shows that Mach number increases with a decrease in the static pressure toward the exit of the nozzle.

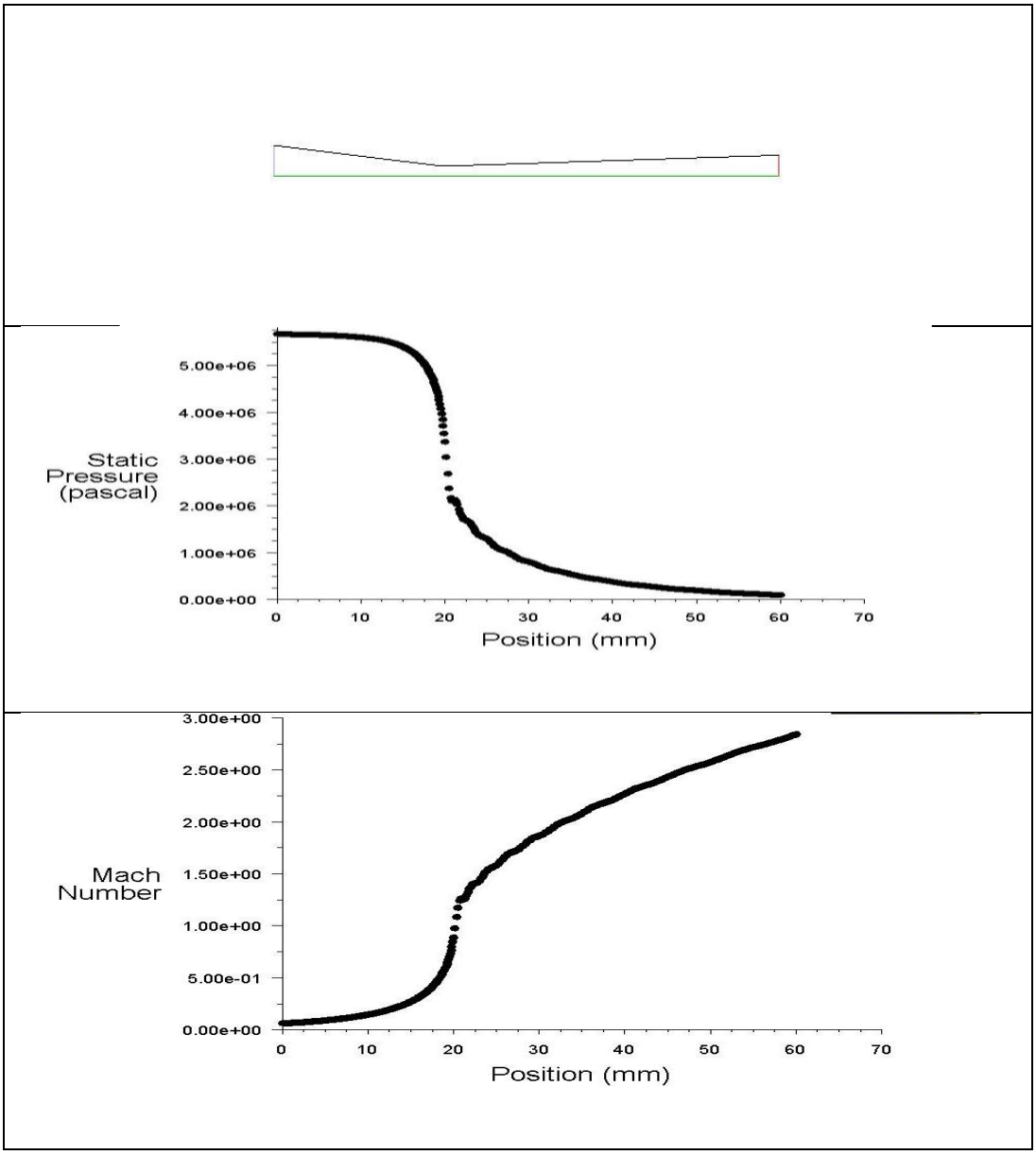

Figure 45: Profile of static pressure and Mach number distribution along the nozzle axis

4.1.1 EFFECT OF PRESSURE AND TEMPERATURE ON VELOCITY OF GAS

The figures below show the velocity of air, nitrogen and helium at the nozzle exit when an applied gas pressure ranging from 1.5 MPa to as high as 3.1 MPa was

used to create the flow field. The stagnation temperature varies from 300 K to 700 K.

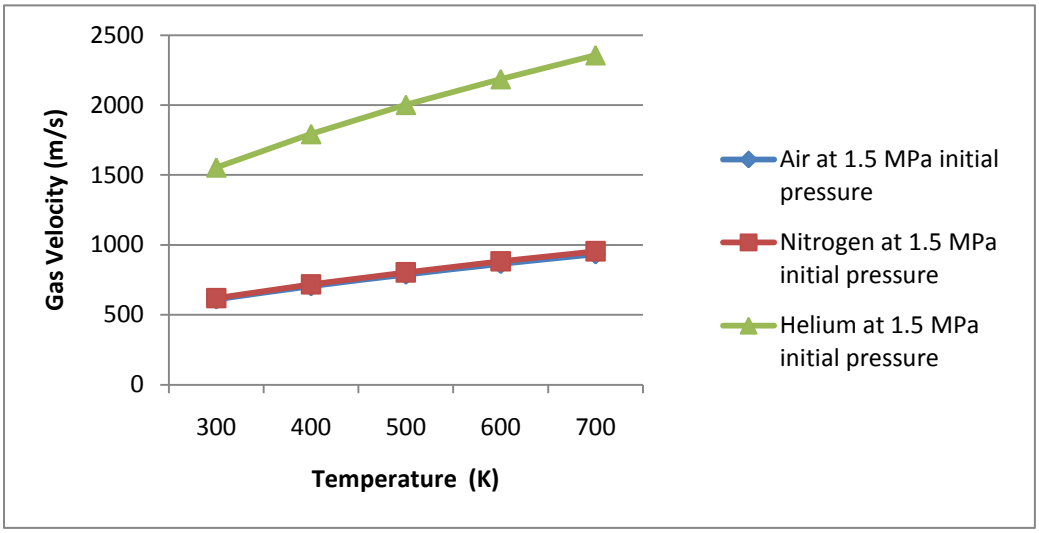

Figure 46: Effect of temperature and on exit velocity when applied gas pressure was 1.5 MPa

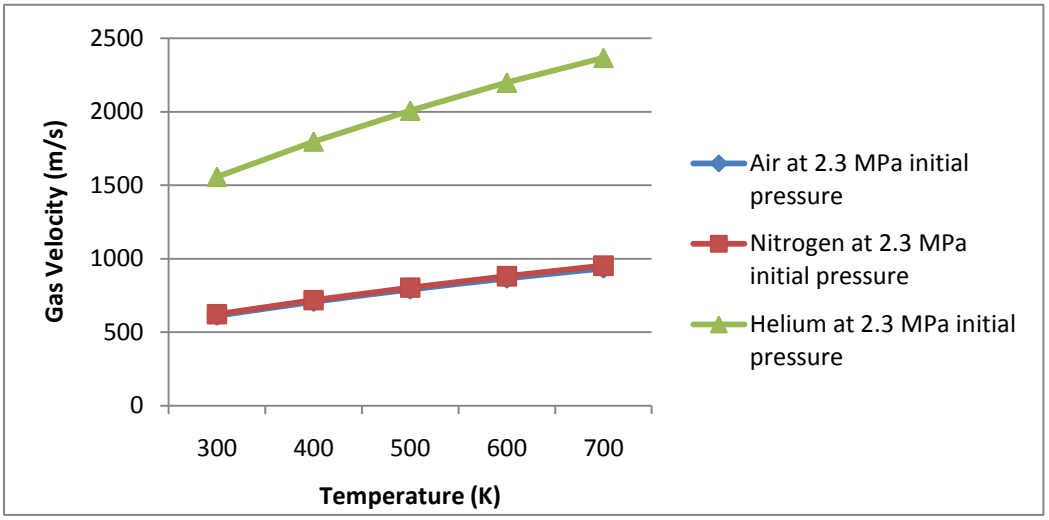

Figure 47: Effect of temperature on exit velocity when applied gas pressure was 2.3 MPa

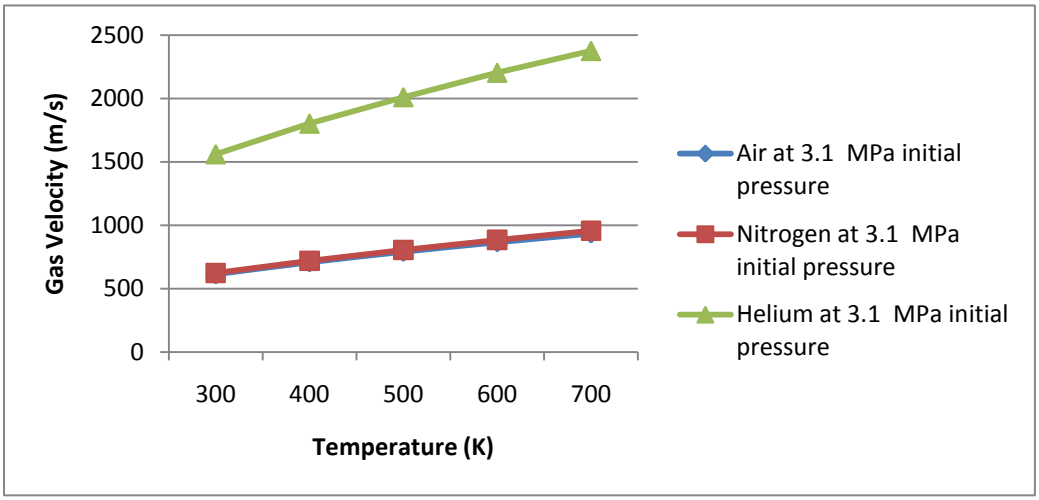

Figure 48: Effect of temperature on exit velocity when applied gas pressure was 3.1 MPa

As the above simulation results show**,** the velocity of air, nitrogen and helium increases with increase in the stagnation temperature from 300 K to 700 K but an applied gas pressure varying from 1.5 MPa to 3.1 MPa did not affect the exit velocity. Figures46, 47 and 48 shows that helium accelerated at almost thrice the velocity of air and nitrogen under the same stagnation conditions of applied pressure and temperature. The gas dynamic equation below explains the reason for the velocity variation with different gases:

$$V_g = M\sqrt{\gamma R T_g}$$

With the nozzle used in simulations, helium attains a higher Mach number than air and nitrogen. For air and nitrogen the specific heat ratio is 1.4 and for helium the specific heat ratio is 1.6. The specific gas constants for air, nitrogen and helium are 287.4 J/Kg K, 296.8 J/Kg K and 2,077 J/Kg K respectively. A conclusion from this is that at the same gas conditions**,** helium will attain a higher gas velocity than air or nitrogen. Also by increasing the inlet gas temperature the gas

velocity will increase and hence result in a higher particle velocity. An increase in gas pressure increases the gas density creating more drag force on the particles which results in a higher particle velocity.

The CFD simulation results using the section above of gas parameters shows that helium is a better accelerating gas than air and nitrogen and can be used for cold spraying**.** However it should be kept in mind that helium is more expensive than nitrogen.

4.2 EFFECT OF TITANIUM PARTICLE SIZE ON EXIT VELOCITY

The previous study on cold spraying showed that density and size of the particles have a significant effect on velocity [47-51]. Settings for carrying out discrete phase modelling (DPM) are presented in appendix 1. In the simulation a titanium particle size ranging from 5 μm to 50 μm was used and air, nitrogen and helium as carrier gases were the accelerant.

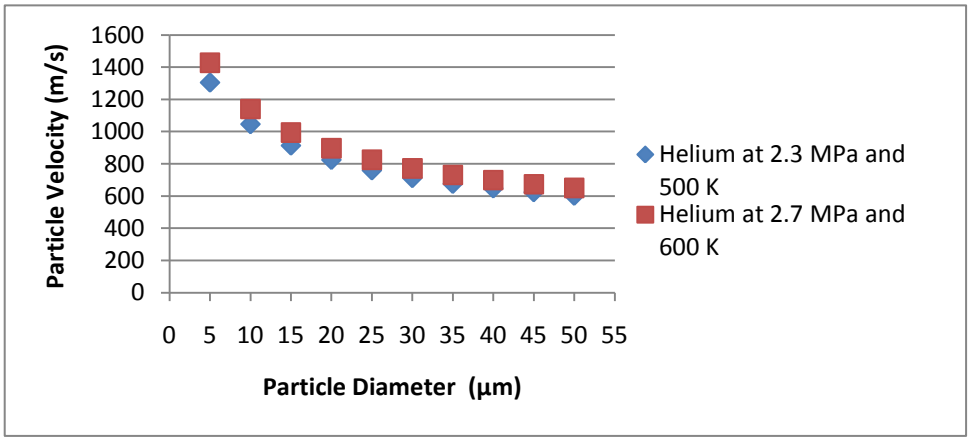

Figure 49: Effect of particle size on its velocity

As the CFD results show**,** smaller particles attain more velocity than larger size particles when helium was used as a carrier gas at 2.3 and 2.7 MPa and a gas temperature of 500 and 600 K. It was notable that the particle velocity increased significantly when the particle size was decreased. Particle in the size range from 5 μm to 20 μm attain a higher velocity than larger titanium particles. An expression for the critical velocity for bonding of spray materials is given by Gartner *et al.* This keeps in mind the mechanical and thermal properties of powder material [25]:

$$V_{crit} = \sqrt{\frac{F_1 4.\sigma_{TS}.\left(1-\frac{T_i - T_R}{T_m - T_R}\right)}{\rho}} + F_2.c_p.(T_m - T_i)$$

ρ is material density, c_p specific heat, T_m melting temperature, T_R reference temperature and T_i impact temperature.

Table 10: Table of thermophysical properties of titanium assumed in simulation are:

Density	4850 Kg/m^3
Specific Heat c_p	544.25 J/Kg-K
Thermal Conductivity	7.44 W/m-K
Electrical Conductivity	2381000 1/ohm-m
Magnetic Permeability	1.257e-06 (h/m)

From the above expression Gartner *et al* found that the critical velocity for titanium particles of size 25 μm was 890 m/s and that the critical velocity is a function of melting temperature hence, by increasing the initial temperature of the carrier gas the critical velocity decreases [25].

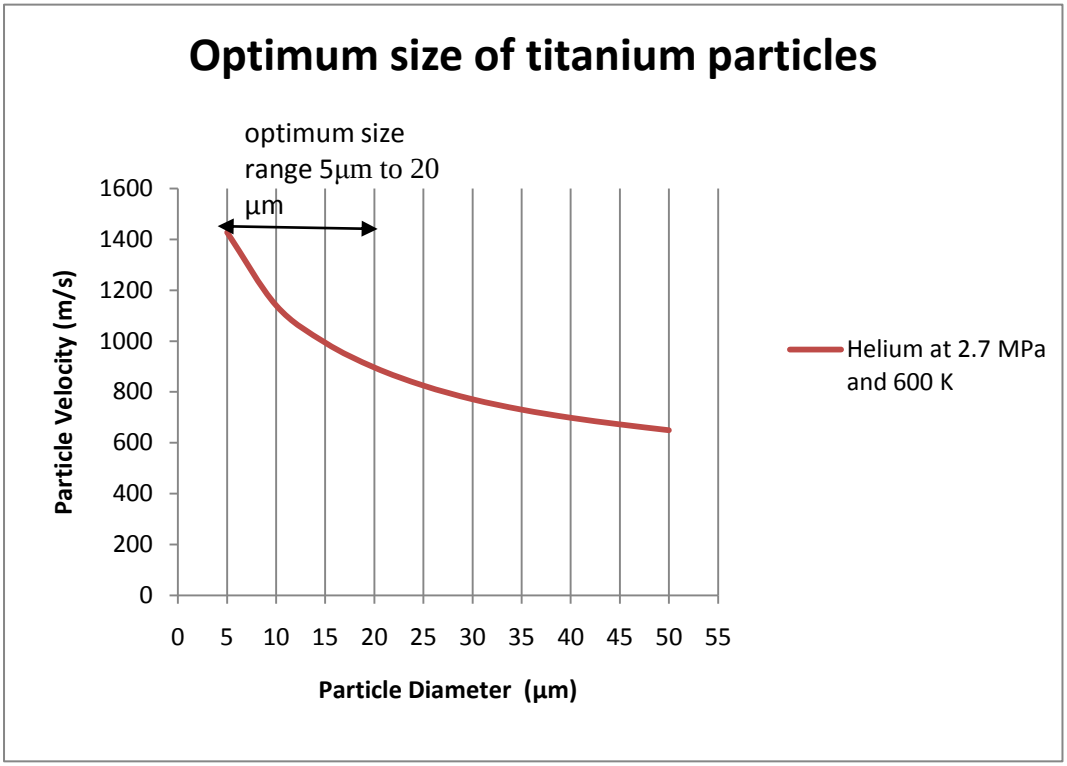

Figure 50: Optimum size range for successful bonding of titanium as spray material

According to the simulation results, titanium particles ranging in size from 5 μm to 20 μm achieve a particle velocity of more than 850 m/s, which is close to the critical velocity for bonding of titanium particles. Hence, particles attaining a velocity greater than the critical velocity can result in more deposition efficiency. Helium was used as a carrier gas with an applied gas pressure of 2.7 MPa and a temperature of 600 K.

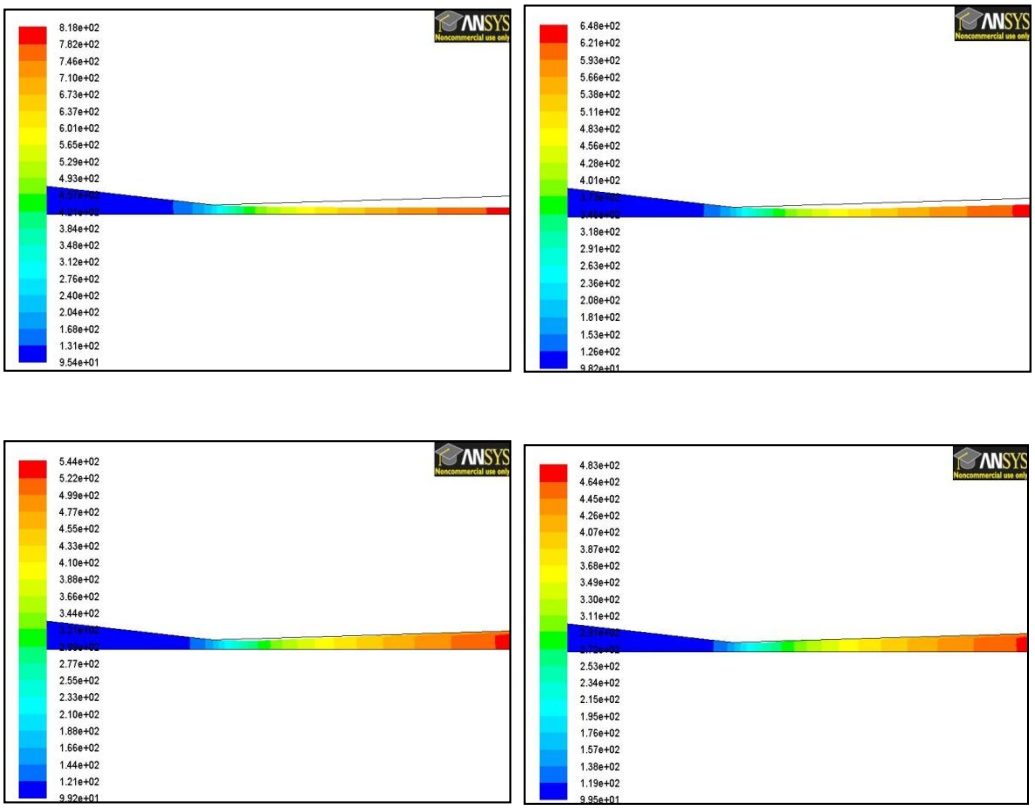

Figure 51: Flow pattern of titanium particles size of 10 µm, 20 µm, 35 µm and 50 µm inside the nozzle using helium as carrier gas at 1.5 MPa and 300 K

The above figures show the flow pattern of the titanium particles inside the nozzle. Simulation results show that titanium particles smaller in size (5 µm to 20 µm) follow the supersonic jet flow of helium gas and the particle stream will strike a small surface area of the substrate**,** which results in a more dense coating.

4.3 EFFECT OF THE CARRIER GAS ON PARTICLE VELOCITY

Three types of gases were used in the simulation to see their affect on the velocity of the titanium particles through the nozzle. The properties of these three gases are presented in Appendix 1.

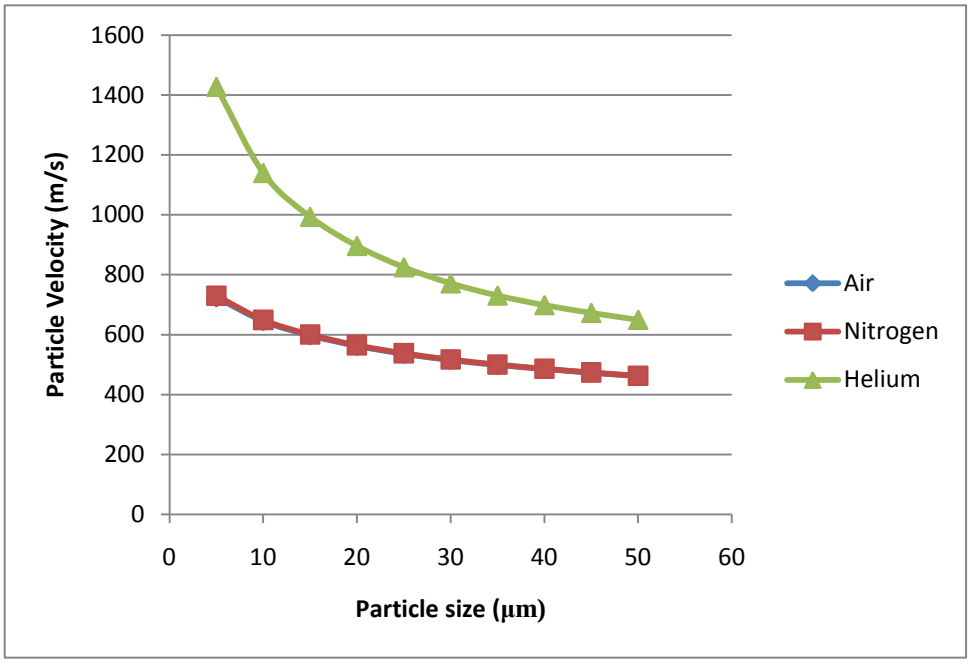

Figure 52: Effect of the carrier gas on titanium particle velocity at applied gas pressure of 2.7 MPa and gas temperature of 600 K

The two dimensional velocity results for titanium particles at the nozzle exit are shown in the figure above when air, nitrogen and helium were used as carrier gases at an applied gas pressure of 2.7 MPa and gas temperature of 600 K. Titanium particles attain more velocity at the exit of the nozzle using helium as a carrier gas compared with nitrogen and air at the same spray conditions. Helium gas attains a higher velocity after passing through the throat than nitrogen or air**.** The results conclude that the low molecular weight, high specific heat ratio,

monoatomic helium gas is a better carrier gas for titanium particles than diatomic air and nitrogen under the same stagnation conditions.

4.4 EFFECT OF GAS CONDITION ON VELOCITY OF TITANIUM PARTICLES

4.4.1 EFFECT OF GAS TEMPERATURE ON PARTICLE VELOCITY

The gas temperature used for simulation ranged from 300 K to 700 K and was used as the stagnation temperature at the nozzle inlet to see the affect of temperature on the velocity of titanium particles.

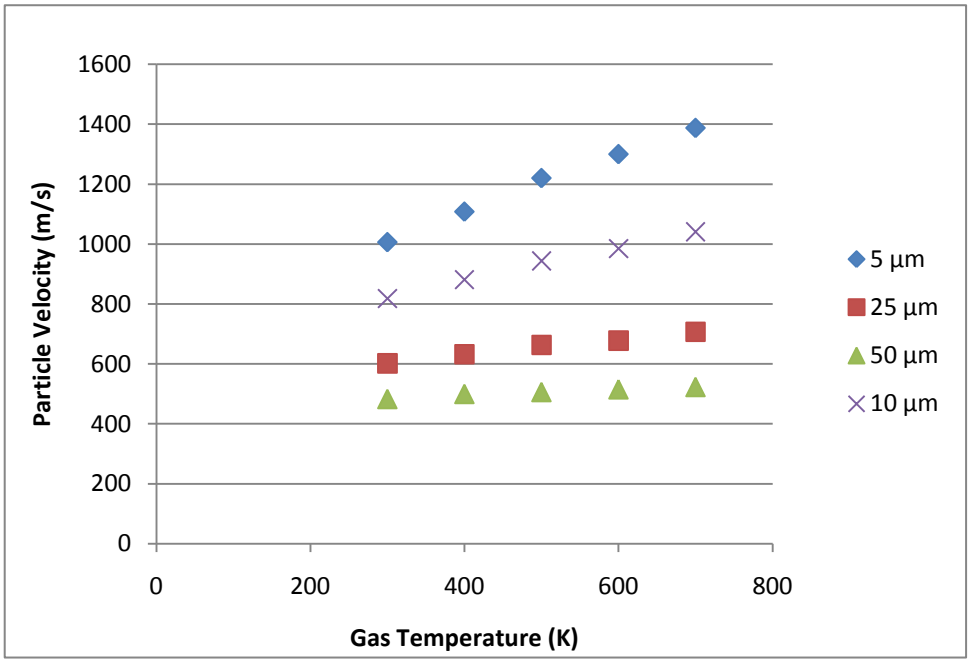

Figure 53: Effect of gas temperature on the velocity of titanium particles

The above figure shows the effect of inlet gas temperature on the velocity of titanium particles when helium was used at 1.5 MPa and a temperature varying from 300 K to 700 K. The simulation results show that by increasing the gas temperature, the sound velocity increases and hence the overall gas velocity

increases, which results in more drag force on the particles. For the smaller titanium particles, size 5 μm to 10 μm**,** the increase in velocity is attributed more to the increase in gas temperature and as the particles get bigger and heavier their velocity does not increase significantly with an increase in gas temperature.

4.4.2 AFFECT OF THE GAS TEMPERATURE ON THE PARTICLE TEMPERATURE

Helium was used as carrier gas in a simulation to see the affect of gas temperature on the particle temperature. The applied gas pressure at the inlet was 1.5 MPa

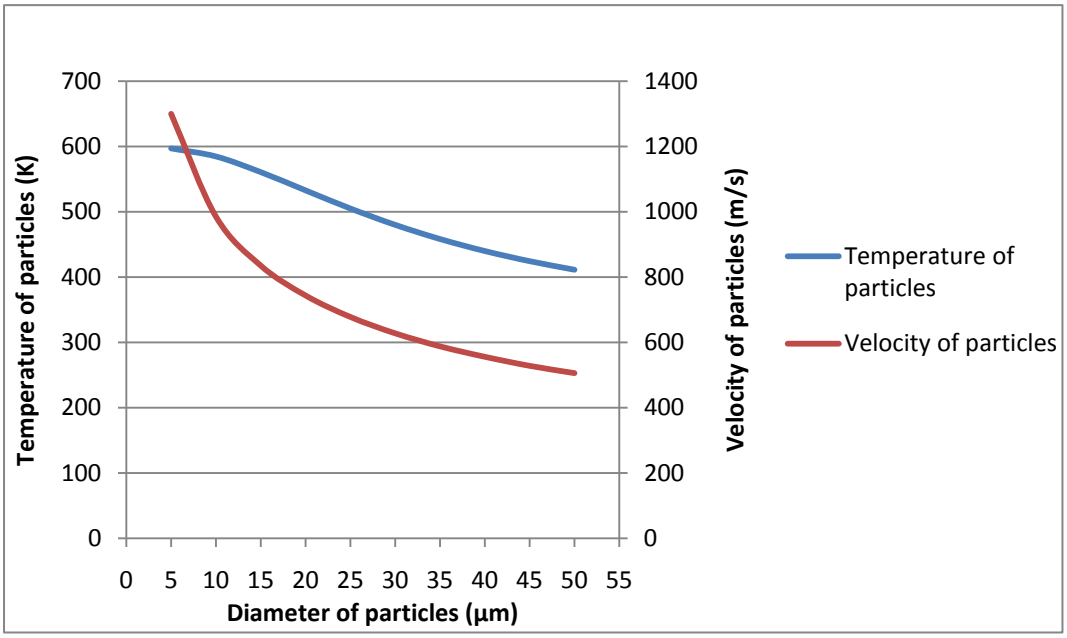

Figure 54: Influence of the particle diameter on the velocity and temperature of the titanium particles

The simulation results show that the particle temperature attains a maximum value at a particle size of 5 μm and decreases with an increase in the titanium particle size. The above results show the relationship for heat transfer between the gas phase and the particle phase. The results show that when helium was used for

spraying titanium particles**,** with an applied pressure of 1.5 MPa and initial temperature of 500 K, the helium gas temperature at the nozzle exit was 114.41 K and the temperature of the titanium particles was 136.23 K, 169.3 K, 205.41 K and 235 .07 K for 5 μm, 10 μm, 15 μm and 20 μm respectively. This shows that the titanium particles were at a higher temperature that the gas in the divergent part of the nozzle when approaching the exit of the nozzle**,** the particles temperature decreased but remained higher than the gas temperature.

Based on the results presented above, increasing the gas temperature increases the particle velocity significantly, which is required for reaching the critical velocity. Gas temperature also influences the temperature of the titanium particles and can help particles to deform after striking the substrate.

4.4.3 AFFECT OF INITIAL PRESSURE ON THE VELOCITY OF TITANIUM PARTICLES

Nitrogen was used as a carrier gas for spraying titanium particles with an inlet gas temperature of 500 K using an applied gas pressure ranging from 1.5 MPa to 3.1 MPa and a titanium particle size ranging from 5 μm to 50 μm.

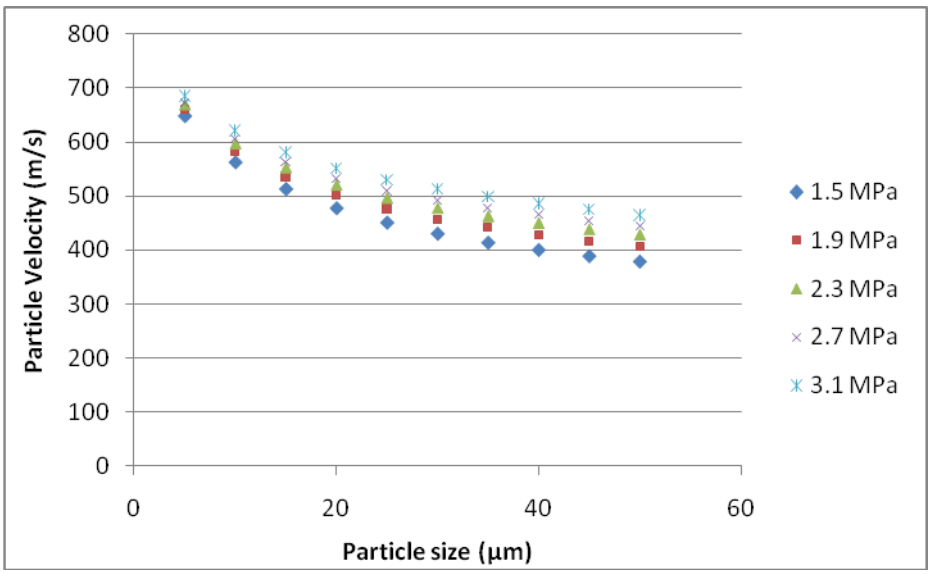

Figure 55: Effect of gas pressure on the particle velocity with different particle size at temperature of 500 K

The results presented in Figure 55 show that changing the gas pressure does not significantly increase the velocity of titanium particles**,** as the velocity of the gas is a function of the total gas temperature according to the isentropic gas flow model. Results show that increasing the gas pressure increases the velocity of larger particles with a size ranging from 35 µm to 50 µm, more than the smaller particles. The reason for a larger particle velocity in bigger titanium particles is explained by the following equation:

$$m_p = \frac{dV_p}{dt} = m_p V_p \frac{dV_p}{dx} = \frac{C_D A_p \rho (V - V_p)^2}{2}$$

where m_p and A_p are the average mass and cross section area of the titanium particles respectively. This equation explains why larger particles accelerate more by increasing initial gas pressure**.** The initial acceleration of titanium particles is a function of the applied gas pressure and not gas temperature. The density of the gas increases by increasing the gas pressure and hence there is more drag force on

the bigger particles resulting in more particle velocity compared with smaller particles.

4.5 EFFECT OF THE NOZZLE DESIGN ON THE VELOCITY OF TITANIUM PARTICLES

Optimising the nozzle design is very important when investigating the cold spraying process along with stagnation conditions, spray particle characteristics and influence of the carrier gas. The geometry of the nozzle was modified to see their affect on the velocity of titanium particles. A model of the nozzle used for simulation is shown below:

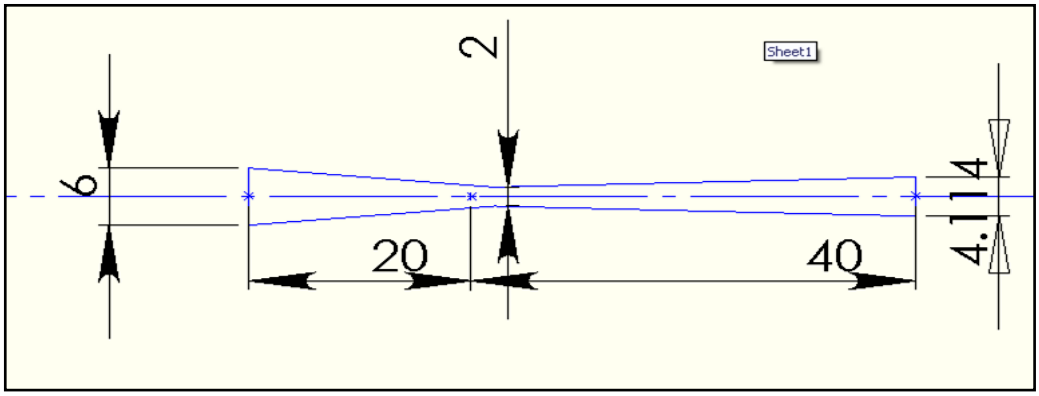

Figure 56: Model of convergent-divergent nozzle used for simulations

4.5.1 EFFECT OF THE DIVERGENT LENGTH

To see the effect of the nozzle divergent length, nitrogen gas was used as a carrier gas for spraying titanium particles at an applied gas pressure of 1.6 MPa and temperature of 600 K.

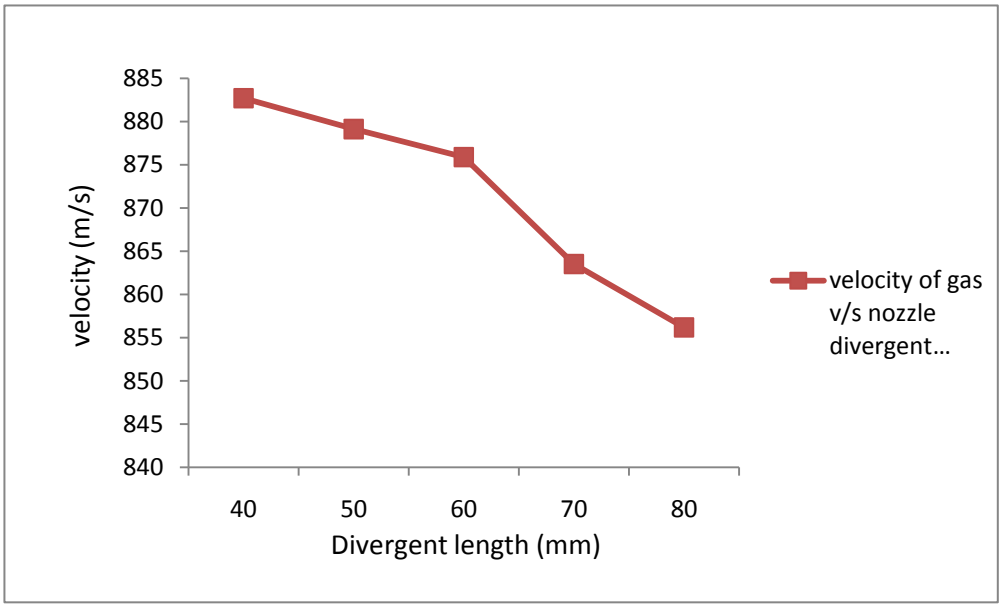

Figure 57: Effect of divergent lengths on the gas velocity

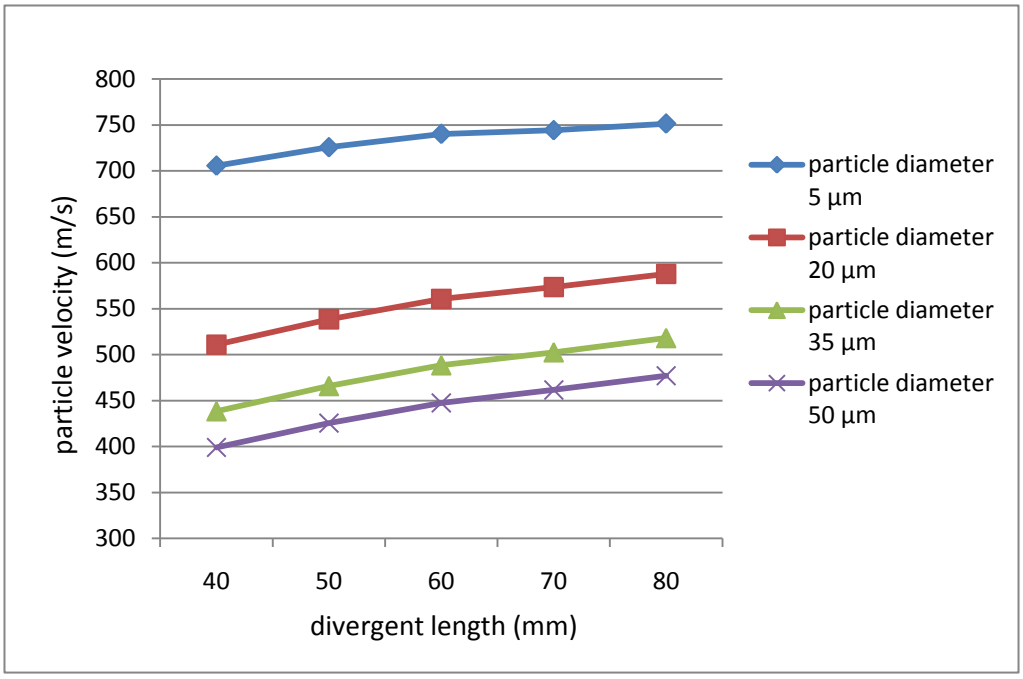

Figure 58: Effect of the nozzle divergent length on the particle velocity

Figure 57 shows that the velocity of gas decreases with an increase in the nozzle divergent length. Because of the longer nozzle divergent section the carrier gas loses its velocity because of frictional losses with the nozzle walls. The effect of

the nozzle divergent length on velocity of titanium particles is shown in Figure 58. The results show that the velocity of titanium particles increases with an increase in the nozzle divergent length from 40 mm to 80 mm. The increase in the velocity of particles with a size of 5 μm was almost 7%, whereas for titanium particles of size 20 μm**,** the increase in the velocity was about 17 %. The equation below shows the relationship between the exit Mach number and the velocity of particles:

$$\sqrt{\frac{\gamma R T_0}{1 + [(\gamma - 1)/2] M^2}}$$

using the equation below the exit Mach number can be calculated for a given exit area:

$$\frac{A}{A_t} = \left(\frac{1}{M}\right)\left[\left(\frac{2}{\gamma + 1}\right)\left(1 + \frac{\gamma - 1}{2} M^2\right)\right]^{(\gamma+1)/[2(\gamma-1)]}$$

The theoretical results are in good agreement with the simulation results showing that by increasing the divergent length the particle velocity **i**ncreases. Also the results show that increasing the nozzle length decreases the gas pressure and this can cause shock inside the nozzle if its length is too large.

4.5.2 EFFECT OF NOZZLE EXIT DIAMETER

Nitrogen gas was used as a carrier gas to spray titanium particles at an applied gas pressure of 2.3 MPa and a gas temperature of 700 K, to see the effect of nozzle exit diameter on the exit velocity of particles. Simulation was done to observe the change in gas velocity and particle velocity when the nozzle exit diameter was changed.

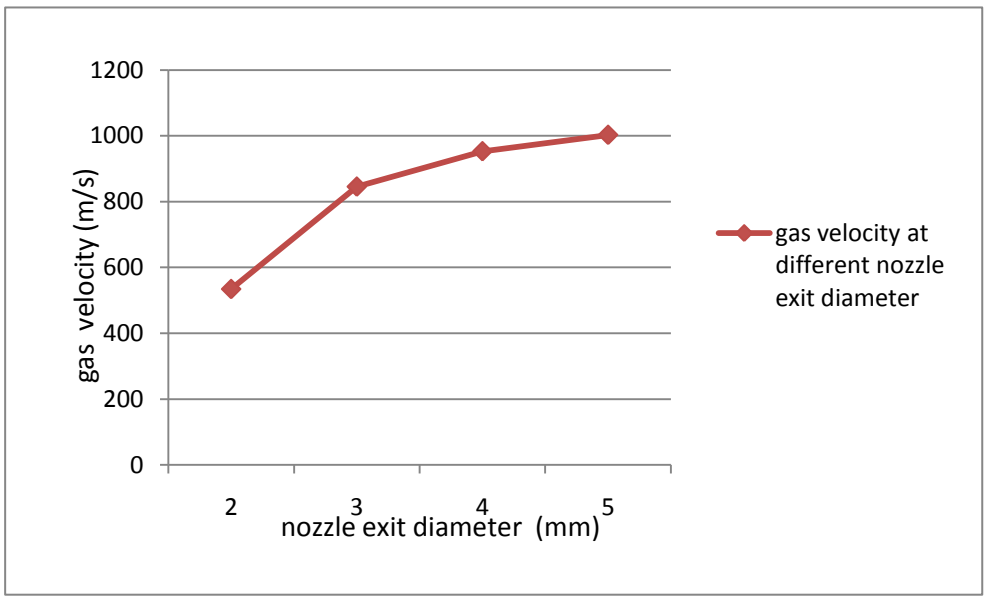

Figure 59: Effect of nozzle exit diameter on the gas velocity

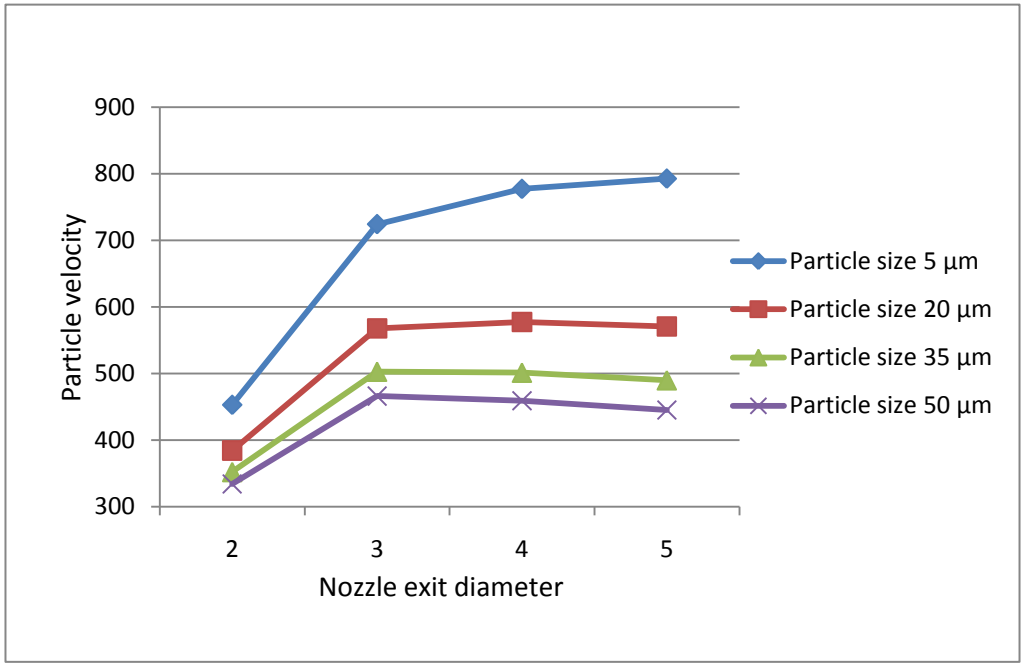

Figure 60: Effect of nozzle exit diameter on the velocity of titanium particles

The simulation results presented in figure 59 show that the nitrogen velocity increased as the nozzle exit diameter was increased from 2 mm to 5mm. The throat diameter was fixed as 2 mm and the exit diameters of the nozzle used in the simulation were 2 mm, 3 mm, 4 mm and 5 mm. The results show that when

titanium particles with sizes ranging from 5 μm to 50 μm were sprayed using nitrogen as a carrier gas the optimum exit diameter decreases from 5 mm to 3 mm with an increase in particle size. Therefore, in a nozzle with a throat diameter of 2 mm and an exit diameter of 4 mm, titanium particles of different sizes can reach a near optimum velocity.

4.6 CONCLUSIONS

The velocity and temperature of titanium particles achieved in a cold spray nozzle were analysed with different nozzle dimensions and different gas process conditions using CFD simulations. The simulation results showed that:

- The Mach number of the gas increases with a decrease in pressure along the axis of the nozzle. This results in greater gas velocity toward the nozzle exit.
- The results show that by increasing the gas temperature the gas velocity increases more significantly than the gas pressure, which shows that the gas velocity is a function of gas temperature and not the gas pressure.
- The results show that the size of titanium particles influences the exit velocity of the particles. As the titanium particle size increased from 5 μm to 50 μm their velocity decreased.
- In the simulation air, nitrogen and helium were used for spraying titanium particles. Results show that helium is a far better carrier gas because particles achieve a much higher velocity when helium is used for spraying. This is twice the velocity achieved when air or helium are used.

- The temperature of the gas influences the velocity of titanium particles because the density of gas decreases with increasing gas temperature and hence there is a greater gas velocity to accelerate the titanium particles
- Increasing the applied gas pressure increases the density of gas which results in more drag on the particles, but increasing the pressure does not significantly affect the particle velocity.
- The results show that by increasing the divergent length of the nozzle the velocity of titanium particles increases.
- The optimum exit diameter of a nozzle was evaluated using different sizes of titanium particles. This showed that titanium particles attain an optimum velocity when the exit diameter of the nozzle is 4 mm.

REFERENCES

1. Tobias Schmidt, Hamid Assadi, Frank Gartner, Horst Richter, Thorsten Stoltenhoff, Heinrich Kreye, and Thomas Klassen, *From Particle Acceleration to Impact and Bonding in Cold Spraying*, Journal of Thermal Spray Technology, JTTEE 18, 2009, p. 794-808

2. Tiziana Marrocco, *Cold Spray Technology from TWI*, TWI Technology Centre (Yorkshire), 2007

3. V.F. Kosarev, S.V. Klinkov, *A.P. Alkhimov, and A.N. Papyrin, On some aspects of gas dynamic of the cold spray process*, ASM international, 2003, JTTEE5 12:265-281

4. J. Karthikeyan, *Cold spray technology: International status and USA efforts*, ASB Industries, Inc., december 2004

5. Global Economy, Advanced materials and processes, April 2008

6. Cold spray technology, http://www.csiro.au/solutions/coldSpray.html, 2009, p. 1-2

7. J. Karthikeyan, *Evolution of cold spray technology*, http://www.entrepreneur.com/tradejournals/article/print/146546589.html, 2010

8. Eric Irissou, Jean-Gabriel Legoux, Anatoly N. Ryabinin, Bertrand Jodoin, and Christian Moreau, *Review on cold spray process and Technology:*

Part 1-Intellectual property, Journal of Thermal Spray Technology, vol 17(4), 2008, p. 495-516

9. P. Fauchais, A. Vardelle, and B. Dussoubs, *Quo Vadis Thermal Spraying*, ASM International, JTTEE 10, 2001, p. 44-66

10. C.-J. Li and A. Ohmori, *Relationships Between the Microstructure and Properties of Thermally Sprayed Deposits*, Journal of Thermal Spray Technology, JTTEE5 11, 2002, p. 365-374

11. H. Singh, B. S. Sidhu, D. Puri, and S. Parkash, *Use of plasma spraying technology for deposition of high temperature oxidation/corrosion resistant coating – a review*, Wiley Inter Science, 2007, p. 92-102

12. ASM International, *Industrial and Research in Thermal Spray Technology in the Nordic region of Europe*, Journal of Thermal Spray Technology, JTTEE5 16, 2007, p. 466-471

13. Cast steel: Advances in Thermal Spray Technology, http://www.keytometals.com/Articles/Art138.htm, 2010, p. 1-2

14. Jin Kawakita a,□, Hiroshi Katanoda b, Makoto Watanabe a, Kensuke Yokoyama a, Seiji Kuroda a, *Warm Spraying: An improved spray process to deposit novel coatings*, Surface & Coating Technology, 202, 2008, p. 4369-4373

15. Thermal spray products, file:///F:/27April/thermalsprayprocesses.html, Metallisation

16. Arc spray process, http://www.gordonengland.co.uk/aws.htm, Surface Engineering Forum

17. Praxair Technology, Inc., *Plasma Spray Process*, Praxair S.T. Technology, Inc., 2005

18. G. D. Davis*, G. B. Groff, R. A. Zatorski, *Plasma Spray Coatings as Treatments for Aluminum, Titanium and Steel Adherends*, Surface and Interface Analysis, VOL. 25, 1997, p. 366-373

19. Rainer Gadow, Andreas Killinger, and Johannes Rauch, *Introduction to High-Velocity Suspension Flame Spraying (HVSFS)*, Journal of Thermal Spray Technology, JTTEE5 17, 2008, p. 655-661

20. Andreas Killinger, Melaine Kuhn, Rainer Gadow, *High-Velocity Suspension Flame Spraying (HVSFS), a new approach for spraying nanoparticles with hypersonic speed*, Elsevier, 201, 2006, p. 1922-1929

21. J. Rauch, G. Bolelli, A. Killinger, R. Gadow, V. Cannillo, L. Lusvarghi, *Advances in High Velocity Suspension Flame Spraying (HVSFS)*, Elsevier, 203, 2009, 2131-2138

22. Sergei Vladimirovich Klinkov, Vladimir Fedorovich Kosarev, Martin Rein, *Cold spray deposition: Significance of particle impact phenomena*, Elsevier, 9, 2005, p. 582-591

23. Anatolii Papyrin, Vladimir Kosarev, Sergey Klinkov, Anatolii Alkhimov, Vasily Fomin, *Cold Spray Technology*, Elsevier, 2007

24. R.C. Dykhuizen and M.F. Smith, *Gas Dynamic Principles of Cold Spray*, Journal of Thermal Spray Technology, JTTEE5 7, 1998, p. 205-212

25. F. Gärtner, T. Schmidt, T. Stoltenhoff and H. Kreye, *Recent Developments and Potential Applications of Cold Spraying*, Wiley Inter Science, 8 no.7, 2006, 611-618

26. Frank Gaertner, Tobias Schmidt, Heinrich Kreye, *Present Status and Future Prospects of Cold Spraying*, Trans Tech Publications, Switzerland, vols. 534-536, 2007, p. 433-436

27. R.E. Blose, B.H. Walker, R.M. Walker, S.H. Jroes, *New opportunities to use cold spray process for applying additive features to titanium alloys*, Elsevier, 2006, p. 30-37

28. Shuo Li, Bary Muddle, Mahnaz Jahedi and Julio Soria, *Numerical Investigation of the Cold Spray Process*, CSIRO, 2009, p.1-6

29. Vladimir F. Kosarev*, Sergey V. Klinkov and Aleksey A. Sova, *Recently Patented Facilities and Applications in Cold Spray Engineering*, Bentham Science Publishers Ltd, 2007, p. 35-42

30. T. Stoltenhoff, H. Kreye, and H.J. Richter, *An Analysis of the Cold Spray Process and Its Coatings,* Journal of Thermal Spray Technology, JTTEE5 11, 2002, p. 542-550

31. T. Han, B.A. Gillispie, and Z.B. Zhao, *An Investigation on Powder Injection in the High-Pressure Cold Spray Process,* Journal of Thermal Spray Technology, JTTEE5 18, 2009, p. 320-330

32. Materials Deposition, Cold Spray, *Department of Defense Manufacturing Process Standard,* AMSC, 2008, 1-14
33. Saden H. Zahiri, William Yang, and Mahnaz Jahedi, *Characterization of cold spray titanium supersonic jet*, Journal of Thermal Spray Technology, JTTEE5 18, 2009, 110-117
34. *Wen-Ya Li and Chang-Jiu Li, Optimal design of a novel cold spray gun nozzle at a limited space,* Journal of Thermal Spray Technology, JTTEE5 14, 2005, 391-396
35. T. Schmidt, F. Gaertner, and H. Kreye, *New Development in Cold Spray Based on Higher Gas and Particle Temperature,* Journal of Thermal Spray Technology, JTTEE5 15, 2006, 488-494
36. M Grujicic, W S DeRosset and D Helfritch, *Flow analysis and nozzle-shape optimization for the cold-gas dynamic-spray process,* ProQuest Science Journals, 217 part B, 2003, p. 1603-1613
37. Wen-Ya Li , Hanlin Liao , Hong-Tao Wang , Chang-Jiu Li , Ga Zhang , C. Coddet, *Optimal design of a convergent-barrel cold spray nozzle by numerical method,* Elsevier, 253, 2006, p. 708-713
38. Chang-Jiu Li*, Wen-Ya Li, *Deposition characteristics of titanium coating in cold spraying,* Elsevier, 167, 2003, 278-283
39. M. Fukumoto, M. Mashiko, M. Yamada, and E. Yamaguchi, *Deposition Behavior of Copper Fine Particles onto Flat Substrate Surface in Cold Spraying,* Journal of Thermal Spray Technology, JTTEE5 19, 2010, 89-94

40. D.L. Gilmore, R.C. Dykhuizen, R.A. Neiser, T.J. Roemer, and M.F. Smith, *Particle Velocity and Deposition Efficiency in the Cold Spray Process,* Journal of Thermal Spray Technology, JTTEE5 8, 1999, 576-582
41. Chang-Jiu Li, Wen-Ya Li, and Hanlin Liao, *Examination of the Critical Velocity for Deposition of Particles in Cold Spraying,* Journal of Thermal Spray Technology, JTTEE5 15, 2006, 212-222
42. T. Van Steenkiste and J.R. Smith, *Evaluation of Coatings Produced via Kinetic and Cold Spray Processes,* Journal of Thermal Spray Technology, JTTEE5 13, 2004, p. 274-282
43. Victor K. Champagne, *The Repair of Magnesium Rotorcraft Components by Cold Spray,* Springer, 2008, p. 164-175
44. T.S. Price, P.H. Shipway, D.G. McCartney, E. Calla, and D. Zhang, *A Method for Characterizing the Degree of Inter-particle Bond Formation in Cold Sprayed Coatings,* Journal of Thermal Spray Technology, JTTEE5 16, 2007, p. 566-570
45. B. Jodoin, F. Raletz, M. Vardelle, *Cold spray modeling and validation using an optical diagnostic method,* Elsevier, 2006, 4424-4432
46. M. Grujicic, C.L. Zhao, C. Tong, W.S. DeRosset, D. Helfritch, *Analysis of the impact velocity of powder particles in the cold-gas dynamic-spray process,* Elsevier, 2004, p. 222-240
47. V. Shukla, G.S. Elliott, and B.H. Kear, *Nanopowder Deposition by Supersonic Rectangular Jet Impingement,* Journal of Thermal Spray Technology, JTTEE5 9, 2000, p. 394-398

48. Chang-Jiu Li, Wen-Ya Li, Yu-Yue Wang, Guan-Jun Yang, H. Fukanuma, *A theoretical model for prediction of deposition efficiency in cold spraying,* Elsevier, 2005, 79-85

49. J.G. Legoux, E. Irissou, and C. Moreau, *Effect of Substrate Temperature on the Formation Mechanism of Cold-Sprayed Aluminum, Zinc and Tin Coatings,* Journal of Thermal Spray Technology, JTTEE5 16, 2007, p. 619-627

50. X. Luo · G. Wang · H. Olivier, *Parametric investigation of particle acceleration in high enthalpy conical nozzle flows for coating applications,* Springer, 2008, 351-362

51. T. Marrocco, D.G. McCartney, P.H. Shipway, and A.J. Sturgeon, *Production of Titanium Deposits by Cold-Gas Dynamic Spray: Numerical Modeling and Experimental Characterization,* Journal of Thermal Spray Technology, JTTEE5 15, 2006, p. 263-272

52. John D. Anderson, *Modern Compressible Flow*, Third Edition, McGraw-Hill Companies, Inc., p. 228-229

53. C. S. JOG, *Fluid Dynamics*, Second Edition, volume-2, Alpha Science International Ltd., p. 412-414

54. B. Jodoin, *Cold Spray Nozzle Mach Number Limitation,* Journal of Thermal Spray Technology, JTTEE5 11, 2002, p. 496-507

55. Cold spray, file://E:\mass flow rate\mm_mp_ct_cs.html, Applied Research Laboratory at Penn State, 2010, p. 1-4

56. M. Grujicic, J.R. Saylor, D.E. Beasley, W.S. DeRosset, D. Helfritch, *Computational analysis of the interfacial bonding between feed-powder*

particles and the substrate in the cold-gas dynamic-spray process, Elsevier Sciences, 219, 200, p. 211-227

57. R. Morgan*, P. Fox, J. Pattison, C. Sutcliffe, W. O'Neill, *Analysis of cold gas dynamically sprayed aluminium deposits*, Elsevier, 58, 2004, p. 1317-1320
58. Wen-Ya Li *, Hanlin Liao, G. Douchy, C. Coddet, *Optimal design of a cold spray nozzle by numerical analysis of particle velocity and experimental validation with 316L stainless steel powder*, Elsevier, 2007, p. 2129-2137
59. J. Vlcek, L. Gimeno, H. Huber, and E. Lugscheider, *A Systematic Approach to Material Eligibility for the Cold-Spray Process*, Journal of Thermal Spray Technology, JTTEE5 14, 2005, p. 125-133
60. R. Nickel, K. Bobzin, E. Lugscheider, D. Parkot, W. Varava, H. Olivier, and X. Luo, *Numerical Studies of the Application of Shock Tube Technology for Cold Gas Dynamic Spray Process,* Journal of Thermal Spray Technology, JTTEE5 16, 2007, p. 729-735
61. Francois Raletz, Michel Vardelle, Guillaume Ezo'o, *Critical Particle Velocity under Cold spray conditions*, Elsevier, 201, 2006, p. 1942-1947
62. T. Stoltenhoff, C. Borchers, F. Ga¨rtner*, H. Kreye, *Microstructures and key properties of cold-sprayed and thermally sprayed copper coatings*, Elsevier, 200, 2006, p. 4947-4960
63. K. Sakaki and Y. Shimizu, *Effect of the Increase in the Entrance Convergent Section Length of the Gun Nozzle on the High-Velocity*

Oxygen Fuel and Cold Spray Process, Journal of Thermal Spray Technology, JTTEE5 10, 2001, p. 487-496

64. Yunus A. Cengel, John M. Cimbala, Fluid Mechanics:- Fundamentals and Applications, chapter 15, p. 860-865

65. H. Katanoda, M. Fukuhara, and N. Iino, *Numerical Study of Combination Parameters for Particle Impact Velocity and Temperature in Cold Spray,* Journal of Thermal Spray Technology, JTTEE5 16, 2007, p. 627-633

66. Taeyoung Han, Zhibo Zhao, Bryan A. Gillispie, and John R. Smith, *Effects of Spray Conditions on Coating Formation by the Kinetic Spray Process,* Journal of Thermal Spray Technology

67. John F. Wendt, *Computational Fluid Dynamics*, Springer, 1996, p 5-6

68. Rainald Lohner, Applied *Computational Fluid Dynamics Techniques*, John Wiley & Sons Ltd., 2001, p 1-2

69. Introduction to Fluent Inc., Chapter 2, 2006, 2-(1-2)

70. B. Samareh, A. Dolatabadi, *A Three-Dimensional Analysis of the Cold Spray Process: Effect of Substrate Location and Shape*, Concordia University, Montreal

71. Y. Li, A. Kirkpatrick, C. Mitchell, B. Willson, *Characteristics and Computational Fluid Dynamics Modelling of High-Pressure Gas Jet Injection*, ASME, vol. 126, January 2004, p. 192-198

72. Sung-Eun Kim and Davor Cokjat, LES is More, Spring, 2005, p 5-7

73. K. Bobzin, E. Lugscheider, R. Nickel, D. Parkot, W. Varava, *A New Concept of the Application of Shock Wave Technology in the Cold Gas Dynamic Spray Process*, RWTH Aachen University

74. J. Pattison, S. Celetto, A. Khan, W. O'Neill, *Standoff distance and bow shock phenomena in the cold spray process*, Elsevier, 2008, p 1443-1454

75. Albert Buxeres I Petipierre, *CFD Simulation of Pressure Loss in Pipes with Different Geometries*, Master Thesis, 2007

76. K. Pougatch, M, salcudean, E. Chan, B. Knapper, *Modelling of Compressible Gas-Liquid Flow in a Convergent-Divergent Nozzle*, Elsevier, vol. 63, 2008, p. 4176-4188

77. K. Taylor, B. Jodoin, and J. Karov, *Particle Loading Effect in Cold Spray*, Journal of Thermal Spray Technology, JTTEE 15, 2006, p 273-279

78. M. Karimi, A. Fartaj, G. Rankin, D. Vanderzwer, W. Birtch, and J. Villafuerte, *Numerical Simulation of the Cold Gas Dynamic Spray Process*, Journal of Thermal Spray Technology, JTTEE 15, 2006, p. 518-523

79. B. Samareh, O. Stier, V. Luthen, and A. Dolatabadi, *Assessment of CFD Modelling via Flow Visualization in Cold Spray Process*, Journal of Thermal Spray Technology, JTTEE 18, 2009, p. 934-943

80. Fluent 6.2 User's Guide, Fluent Inc., Lebanon, NH, 2005

81. http://www.cfd-online.com/Wiki/Sutherland_law

APPENDIX 1

The computational values used for simulation in Fluent are presented in table below. The values not specified were used as default:

BOUNDARY CONDITIONS

INLET BOUNDARY CONDITIONS	
Boundary Type	Mass Flow Rate
Direction Specification Method	Normal to Boundary
Operating Pressure	0
Reference Frame	Absolute
Turbulence Specification Method	Intensity and Length Scale
Turbulence Intensity	1%
Turbulence Length Scale	20% of Nozzle Inlet Diameter

OUTLET BOUNDARY CONDITIONS	
Boundary Type	Pressure Outlet
Gauge Pressure	0
Direction Specification Method	From Neighbouring Cells

Turbulence Specification Method	Intensity and Length Scale
Backflow Turbulence Intensity	1%
Backflow Turbulence Length Scale	20% of Nozzle Inlet Diameter

DISCRETE PHASE MODELLING	
Injection Type	Surface
Release From Surface	Inlet
Material	Titanium
Diameter Distribution	Uniform
Drag Law	Spherical
Initial Particle Temperature	300 K
Velocity Magnitude	100 m/s
Particle diameter	5,10,15,20,25,30,35,40,45,50 μm
Total Mass Flow Rate	0.001 Kg/s

APPENDIX 2

Mass flow rate was used as inlet boundary condition for the simulation of cold spray nozzle. Hence, isentropic one-dimensional model was used to calculate mass flow rate which exerts the initial pressure for acceleration of gas through convergent-divergent nozzle.

Firstly, temperature at throat T_t was calculated using the equation 1 below:

$$\frac{T_0}{T_t} = \frac{2}{2 + (\gamma - 1)M_t}$$

Here γ is specific heat ratio. For helium γ is 1.66 and for air and nitrogen γ is 1.4. T_0 is the total temperature in equation 1. Mach number at throat M_t was assumed to be unity.

The density of gas inside chamber ρ_0 was calculated as:

$$\rho 0 = \frac{P_0}{RT_0}$$

The density at throat ρ_t:

$$\frac{\rho_t}{\rho_0} = \left[\frac{2}{2 + (\gamma - 1){M_t}^2}\right]^{1/\gamma - 1}$$

At throat the local velocity V_t can be calculated by:

$$Vt = \sqrt{\gamma R T_t}$$

where R is the specific gas constant and value of R is:

R for air = 0.287 KPa.m^3/Kg. K

R for nitrogen = 0.296 KPa.m^3/Kg. K

R for helium = 2.077 KPa.m^3/Kg. K

Mass flow rate $\dot{m}$ at throat can be calculated by:

$$\dot{m} = \rho_t A_t V_t$$

where A_t is the throat diameter